



# LUND UNIVERSITY

## Non-invasive diagnostic methods of intracranial arteries

Ramgren, Birgitta

2014

[Link to publication](#)

*Citation for published version (APA):*

Ramgren, B. (2014). *Non-invasive diagnostic methods of intracranial arteries*. [Doctoral Thesis (compilation), Diagnostic Radiology, (Lund)]. Diagnostic Radiology, (Lund).

*Total number of authors:*

1

### General rights

Unless other specific re-use rights are stated the following general rights apply:

Copyright and moral rights for the publications made accessible in the public portal are retained by the authors and/or other copyright owners and it is a condition of accessing publications that users recognise and abide by the legal requirements associated with these rights.

- Users may download and print one copy of any publication from the public portal for the purpose of private study or research.
- You may not further distribute the material or use it for any profit-making activity or commercial gain
- You may freely distribute the URL identifying the publication in the public portal

Read more about Creative commons licenses: <https://creativecommons.org/licenses/>

### Take down policy

If you believe that this document breaches copyright please contact us providing details, and we will remove access to the work immediately and investigate your claim.

LUND UNIVERSITY

PO Box 117  
221 00 Lund  
+46 46-222 00 00

# Non-invasive diagnostic methods of intracranial arteries

Birgitta Ramgren



**LUND**  
UNIVERSITY

DOCTORAL DISSERTATION

by due permission of the Faculty of Medicine, Lund University, Sweden.  
To be defended at demonstration room 10, Department of Medical Imaging and  
Physiology, Main building, level 4, Skåne University Hospital, Lund  
Friday 13<sup>th</sup> of June 2014, 13.00


*Faculty opponent*

Professor Sven Ekholm

Department of Radiology, University of Gothenburg

Organization LUND UNIVERSITY Department of Diagnostic Radiology Clinical Sciences, Faculty of Medicine	Document name DOCTORAL DISSERTATION	
	Date of issue June 13, 2014	
Author: <b>Birgitta Ramgren</b>	Sponsoring organization	
<b>Title: Non-invasive diagnostic methods of intracranial arteries</b>		
<b>Abstract</b> Aims of this thesis were to compare the agreement of different magnetic resonance angiography (MRA) techniques and digital subtraction angiography (DSA) in follow-up of intracranial aneurysms treated with coils in order to select the best MRA method, to evaluate the impact of increased iodine concentration in contrast medium and decreased tube voltage on arterial attenuation and image quality in computed tomography angiography (CTA) of intracranial arteries, and finally to evaluate the diagnostic accuracy of CTA in non-traumatic subarachnoid haemorrhage (SAH) compared to DSA and to assess the arterial attenuation (HU) as an image quality factor in this aspect. Follow-up DSA and time-of-flight (TOF) MRA at 1.5T and 3T as well as contrast-enhanced MRA at 3T were performed in 37 patients with 41 coiled intracranial aneurysms. TOF-MRA at 3T showed best agreement with DSA. One of three different combinations of iodine concentrations in contrast medium and CT tube voltages was tested in each of 63 patients referred for CTA of intracranial arteries. Increased iodine concentration (400 mgI/ml) and decreased tube voltage (90 kVp) improved image quality in CTA of intracranial arteries and arterial attenuation at 340 HU in the ICA was found to represent a cut-off level for examinations of good quality. In 326 patients with non-traumatic SAH, diagnostic accuracy and arterial attenuation (HU), reflecting image quality, were assessed for CTA. CTA can be performed with high sensitivity (95%) and specificity (97%) for detection of ruptured aneurysms in the acute setting of SAH and arterial attenuation is correlated to the sensitivity.		
<b>Key words:</b> intracranial aneurysms; endovascular treatment; follow-up; subarachnoid haemorrhage; digital subtraction angiography; magnetic resonance angiography; computed tomography angiography; technical aspects; contrast agents; image quality		
Classification system and/or index terms (if any)		
Supplementary bibliographical information	Language: English	
ISSN and key title; 1652-8220 Non-invasive diagnostic methods of intracranial arteries		ISBN 978-91-87651-90-8
Recipient's notes	Number of pages 116	Price
	Security classification	

I, the undersigned, being the copyright owner of the abstract of the above-mentioned dissertation, hereby grant to all reference sources permission to publish and disseminate the abstract of the above-mentioned dissertation.

Signature  Date April 28, 2014

# Non-invasive diagnostic methods of intracranial arteries

Birgitta Ramgren



**LUND**  
UNIVERSITY

Department of Diagnostic Radiology,  
Clinical Sciences Lund, Faculty of Medicine,  
Lund University and Skåne University Hospital  
2014



Cover images: Patient with an ACOM aneurysm, where the large image shows CTA (volume rendering) before treatment and small images (from upper to lower image) 3D and 2D DSA before treatment with coils, 2D DSA directly after treatment and one year after treatment, follow-up with TOF-MRA at 3T showing susceptibility artefact (MPR) and occlusion of the aneurysm (MIP). (*Author images*)

Thesis for degree of Doctor of Philosophy in Medical Science  
© Birgitta Ramgren, 2014

Department of Diagnostic Radiology, Clinical Sciences Lund, Faculty of Medicine,  
Lund University and Skåne University Hospital

Lund University, Faculty of Medicine Doctoral Dissertation Series 2014: 64  
ISBN 978-91-87651-90-8  
ISSN 1652-8220

Printed in Sweden by Media-Tryck, Lund University  
Lund 2014



To Jens



# Contents

<b>Abbreviations</b>	9
<b>Thesis at a glance</b>	11
<b>Original papers</b>	13
<b>Populärvetenskaplig sammanfattning</b>	15
Bakgrund	15
Diagnostik av pulsåderbräck på hjärnans kärl	15
Radiologiska tekniker	15
Delarbetens huvudmål och slutsatser	16
Implementering av delarbetens slutsatser i den kliniska verksamheten	17
<b>Introduction</b>	19
<b>Background</b>	21
Historical background	21
Anatomy	22
Circle of Willis	22
Imaging methods	23
Digital subtraction angiography	23
Magnetic resonance angiography	24
Computed tomography angiography	25
General technical considerations	26
Pathology	26
Aneurysms	26
Cerebral vascular malformations	28
Other vascular diseases of the brain	30
Subarachnoid haemorrhage	33
Treatment of intracranial aneurysms	35
Background for study initiation	38
Paper I	38
Paper II	39
Paper III	39
<b>Aims</b>	41
Paper I	41

Paper II	41
Paper III	41
<b>Methods</b>	<b>43</b>
Ethics	43
DSA technique	43
MRA technique	43
CTA technique	44
Study groups and main methods	45
Data evaluation	45
Paper I	45
Paper II	46
Paper III	47
Statistical analysis	47
Paper I	47
Paper II	48
Paper III	48
<b>Results</b>	<b>49</b>
Paper I	49
Paper II	50
Paper III	52
<b>Discussion</b>	<b>57</b>
Main findings	57
Inclusion criteria	57
DSA as gold standard	58
Contrast agents	59
Image evaluation	59
Grading scales	61
Image quality grading	61
Clinical implications	63
Future aspects	63
<b>Conclusions</b>	<b>65</b>
Paper I	65
Paper II	65
Paper III	65
<b>Recommendations and impact on clinical routine</b>	<b>67</b>
<b>Acknowledgements</b>	<b>69</b>
<b>References</b>	<b>71</b>
<b>Paper I-III</b>	

# Abbreviations

ACA	Anterior cerebral artery
ACOM	Anterior communicating artery
AICA	Anterior inferior cerebellar artery
AVM	Arteriovenous malformation
BA	Basilar artery
CE-MRA	Contrast-enhanced magnetic resonance angiography
CT	Computed tomography
CTA	Computed tomography angiography
CTDI <sub>vol</sub>	Computed tomography dose index
dAVF	Dural arteriovenous fistula
DLP	Dose length product
DSA	Digital subtraction angiography
HU	Hounsfield units
ICA	Internal carotid artery
kVp	Kilovolt peak
mAs <sub>eff</sub>	Effective millampere second
MCA	Middle cerebral artery
mgI/ml	Milligram iodine/millilitre
mGy	Milligray
MIP	Maximum intensity projection
MPR	Multi-planar reconstruction
MRA	Magnetic resonance angiography
MRI	Magnetic resonance imaging

PA	Pericallosal artery
PACS	Patient Archiving and Communication System
PCA	Posterior cerebral artery
PCOM	Posterior communicating artery
PICA	Posterior inferior cerebellar artery
RIS	Radiology Information System
ROI	Region of interest
SAH	Subarachnoid haemorrhage
SCA	Superior cerebellar artery
SD	Standard deviation
T	Tesla
TOF-MRA	Time-of-flight magnetic resonance angiography
VR	Volume rendering
2D	two-dimensional
3D	three-dimensional

# Thesis at a glance

Paper	I	II	III
<b>Aims</b>	To compare the agreement between TOF-MRA and CE-MRA at 3T and TOF-MRA at 1.5T with DSA for the follow-up of intracranial aneurysms treated with detachable coils in order to select the best MRA method.	To evaluate the impact of increased iodine concentration in contrast medium from 300 to 400 mgI/ml and the effect of decreased tube voltage from 120 to 90 kVp on image quality and arterial attenuation in CTA of intracranial arteries.	To evaluate the diagnostic accuracy of CTA in non-traumatic SAH compared to DSA and to assess the arterial attenuation (HU) as an image quality factor in this aspect.
<b>Methods</b>	41 aneurysms in 37 patients treated with endovascular coiling and scheduled for follow-up DSA to assess the grade of occlusion. The patients also performed MRA at 1.5T (TOF-MRA) and at 3T (TOF-MRA and CE-MRA) to compare with DSA.	63 patients referred for CTA of intracranial arteries, were included in three groups with a combination of different iodine concentration of contrast medium and tube voltage to compare image quality and arterial attenuation (HU).	326 patients with non-traumatic SAH who underwent CTA and DSA were included and aneurysm detection per patient, per aneurysm and per ruptured aneurysm was done. Measurements were performed of arterial attenuation (HU) as an image quality factor.
<b>Results</b>	TOF-MRA at 3T shows better agreement with DSA regarding aneurysms treated with coils than TOF-MRA at 1.5T and CE-MRA 3T.	Arterial attenuation (HU) in ICA was higher with high iodine concentration in contrast medium. Reduced tube voltage raised arterial enhancement. The combination of the two improved image quality.	285 aneurysms were found, 19 of which were missed on CTA. Correct diagnosis with CTA in 28 patients with perimesencephalic haemorrhage. A significant difference was seen between true positive and true negative aneurysms compared with false negative regarding arterial attenuation (HU).
<b>Conclusion</b>	MRA, being a non-invasive method and without using ionizing radiation, can be used for follow-up of aneurysms treated endovascularly with coils. TOF-MRA at 3T is superior to the other two tested MRA settings.	The use of highly concentrated contrast medium and low tube voltage improves image quality in CTA of intracranial arteries.	CTA has a high sensitivity and specificity for detection of ruptured aneurysms and arterial attenuation is correlated to the sensitivity.





# Original papers

This thesis is based on the following papers, which will be referred to in the text by their Roman numerals I – III. The complete papers are appended at the end of the thesis.

- I. B. Ramgren, R. Siemund, M. Cronqvist, P. Undrén, O.G. Nilsson, S. Holtås, E-M. Larsson  
Follow-up of intracranial aneurysms treated with detachable coils: comparison of 3D inflow MRA at 3T and 1.5T and contrast-enhanced MRA at 3T with DSA  
*Neuroradiology* 2008 Nov; 50(11):947-544
  
- II. B. Ramgren, I.M. Björkman-Burtscher, S. Holtås, R. Siemund  
CT angiography of intracranial arterial vessels: impact of tube voltage and contrast media concentration on image quality  
*Acta Radiologica* 2012 Oct; 53:929-934
  
- III. B. Ramgren, R. Siemund, O.G. Nilsson, P. Höglund, E-M. Larsson, K. Abul-Kasim, I.M. Björkman-Burtscher  
CT angiography in non-traumatic subarachnoid haemorrhage: The importance of arterial attenuation for detection of intracranial aneurysms  
Submitted to *Acta Radiologica*. Manuscript ID SRAD-2014-0342



# Populärvetenskaplig sammanfattning

## Bakgrund

Icke-traumatisk hjärnhinneblödning (SAH) kan orsakas av ett brutet pulsåderbräck (aneurysm) och är ett allvarligt tillstånd. Ett pulsåderbräck utgörs av en försvagning av kärlväggen och det finns ett pulsåderbräck på hjärnans kärl hos cirka 2 % av befolkningen. Det är inte alla pulsåderbräck som brister, utan detta sker hos cirka 6-9 personer i en population på 100 000 invånare d.v.s. i södra sjukvårdsregionens upptagningsområde på 1,7 miljoner invånare cirka 100-150 patienter om året.

## Diagnostik av pulsåderbräck på hjärnans kärl

Då en patient misstänks ha hjärnhinneblödning, utreds patienten i första hand med datortomografi av skallen (CT) samt datortomografi av hjärnans kärl (CTA) för att bekräfta eller utesluta pulsåderbräck eller annan kärlsjukdom. Vid osäkerhet utförs även konventionell kärlröntgen (DSA).

Vid utredning av patienter med misstanke om pulsåderbräck utan hjärnhinneblödning görs oftast magnetkameraundersökning av hjärnans kärl (MRA).

Patienter som behandlas för pulsåderbräck med små metallspiraler s.k. coils, behöver kontrolleras med kärlröntgen för att se att pulsåderbräcket är stängt och skyddat mot blödning. Detta gjordes tidigare med konventionell kärlröntgen, men numera med magnetkameraundersökning.

## Radiologiska tekniker

Konventionell kärlröntgen innebär att patienten måste vara inlagd på sjukhus, i dagsläget under dagen. Undersökningen utförs på röntgenavdelningen och patienten kläs in i sterila lakan. Röntgenläkaren ger lokalbedövning i ljumsken, ett litet stick i pulsådern och sedan för man in en slang (kateter) i kärlet för att un-

dersöka hjärnans kärl med kontrastmedel via halskärlen. Undersökningen tar cirka 20-60 minuter.

Vid datortomografi av hjärnans kärl, kan patienten komma på en avtalad tid och en liten slang läggs in i ett kärl i armvecket, där kontrastmedlet ges. Själva bildtagningen tar några sekunder.

Undersökning av hjärnans kärl med magnetkamera kan göras dels utan tillförsel av kontrastmedel s.k. inflödesteknik (TOF-MRA) samt med tillförsel av kontrastmedel (CE-MRA), det sistnämnda sker på samma sätt som vid datortomografin. Tiden för bildtagning är vid kontrastförstärkt undersökning cirka 1 minut och för inflödesteknik 5-8 minuter. MR består av flera bildtagningsomgångar, varav kärlundersökningen är en av dem.

## Delarbetens huvudmål och slutsatser

I det *första delarbetet* görs en bedömning av vilken metod och fältstyrka (mätt i Tesla, T) på magnetkameran som bäst överensstämmer med konventionell kärldröntgen (referensundersökning), avseende patienter med pulsåderbräck på hjärnans kärl som har behandlats med coils. Detta delarbete visade att undersökningar utförda med s.k. inflödesteknik på en magnetkamera med fältstyrkan 3T hade bäst överensstämmelse med konventionell kärldröntgen jämfört med inflödesteknik på 1.5T och kontrastförstärkt magnetkameraundersökning på 3T. Denna slutsats har senare bekräftats i andra studier.

I *delarbete två* ingår optimering av bildkvalitet för undersökning av hjärnans kärl på datortomografi avseende kontrastmedel och rörspänning. Vid kombinationen hög jodhalt i kontrastmedlet (400 mgI/ml) och låg rörspänning (90 kVp) blev bildkvaliteten bedömd som bättre jämfört med övriga grupper (300 mgI/ml och 120 kVp respektive 400 mgI/ml och 120 kVp). Avseende bildkvalitet visas att hög strålabsorptionsförmåga av de kontrastfyllda inre halspulsåderna (ICA) med ett absorptionsvärde över 340 HU gav bilder av standard eller utmärkt kvalitet i 90 % av undersökningarna.

I det *tredje delarbetet* undersöktes känsligheten och tillförlitligheten avseende diagnosen av pulsåderbräck på patienter med icke-traumatisk hjärnhinneblödning vid undersökning av hjärnans kärl med datortomografi. Som referensundersökning användes konventionell kärldröntgen och känsligheten att hitta ett brustet pulsåderbräck är 95 % och tillförlitligheten är 97 % på CTA. Detta är i överensstämmelse med andra publicerade studier. Dessutom visade studien att känsligheten avseende diagnostik av pulsåderbräck på datortomografi av hjärnans kärl är relaterad till det objektiva kvalitetsmättet på absorptionsvärde som togs fram i artikel två.

## Implementering av delarbetens slutsatser i den kliniska verksamheten

Avseende patienter med pulsåderbräck som är behandlade med coils, görs numera uppföljande kontrollundersökningar med magnetkamera och inflödesteknik och företrädesvis en fältstyrka på 3T.

Vid undersökning av hjärnans kärl med datortomografi används hög jod koncentration i kontrastmedlet i kombination med låg rörspänning.

Hos patienter med icke-traumatisk hjärnhinneblödning, där datortomografin av hjärnans kärl är av god kvalitet eller ett pulsåderbräck påvisas, bedöms utredningen som fullgod och behandlingsbeslut kan tas. Det objektiva kvalitetsmättet kan användas som stöd i bedömningen av undersökningskvalitén. Om undersökningen är av dålig kvalitet, görs en förnyad datortomografi eller en konventionell kärldröntgen.



# Introduction

Intracranial aneurysms develop in the cerebral arteries because of a focal weakness of the arterial wall and mostly aetiology is unknown. The prevalence of intracranial aneurysms in the general population is approximately 2% (0.2-9%)<sup>1</sup>. Most aneurysms do not rupture and the incidence of aneurysmal subarachnoid haemorrhage (SAH) in the western population is approximately 6-9 per 100 000<sup>2,3</sup> except in Finland, where rates are 2-3 times higher<sup>4</sup>.

Aneurysm rupture with SAH has a fatal outcome in the acute phase in between 32%-67% of cases (between 1960 and 1992)<sup>5</sup> however, mortality rates in hospital have decreased over the years from reported 17% between 1973 and 2002<sup>6</sup> to 9.8% 2007<sup>7</sup>. The decrease in case-fatality is explained by a combination of different factors such as more accurate and especially faster first line diagnostic tools (e.g. computed tomography angiography, CTA and magnetic resonance imaging, MRI) and the improvement of neuroanaesthesia and intensive-care managements as well as the increased availability of surgical and endovascular treatments<sup>7,8</sup>.

The latter underlines the importance of pre-therapeutic diagnostic angiographic methods that are fast and safe and with high sensitivity and specificity. Also the possibility to predetermine which aneurysm has ruptured or is at risk to rupture is important, since all aneurysms do not rupture. Demographic factors as age, gender, ethnicity and previous SAH have an impact on rupture risk as well as the location, size and whether there are multiple aneurysms<sup>2,9</sup>.

Digital subtraction angiography (DSA) is a diagnostic modality with high sensitivity and specificity to detect intracranial aneurysms, used as gold standard, but it is an invasive and time consuming technique with a risk of symptomatic complication 0.5-2% of cases<sup>10-12</sup>, however at dedicated high-volume neurointerventional centre, a risk rate as low as 0.06% has been reported<sup>13</sup>.

CTA is a well-established method for fast and non-invasive evaluation of intracranial aneurysms. Due to the development of CT techniques e.g. from single to multislice technique (4 to 128- slice) and 320 detector-row CT, the modality has become fast and easily accessible, therefore often the first diagnostic choice in clinical practice. Further technical developments such as bone-removal of the skull base, either by subtraction of two CT scans or by dual-source CTA are being developed and introduced in the clinical routine<sup>14-17</sup>.



MRA is a non-invasive technique without ionizing radiation for detection of intracranial aneurysms but has limitations especially for evaluation of small aneurysms and aneurysms located at the skull base<sup>18</sup>. It can be performed as contrast-enhanced (CE-MRA) technique using gadolinium-based contrast medium or by using the time-of-flight technique (TOF-MRA)<sup>19-21</sup>.

This thesis is based on studies addressing different diagnostic methods of intracranial arteries focusing on non-invasive MRA at different field strengths and utilizing contrast-enhanced and non-contrast-enhanced MRA techniques, optimization and image quality of CTA, as well as assessment of clinical routine aneurysm detection and its correlation to image quality by considering arterial attenuation (HU) as a quality parameter.

# Background

## Historical background

In 1927, the first cerebral angiogram was performed by E Moniz, professor in neurology, Lisbon. The application in clinical practice was published in *Lancet* 1933 after 300 angiograms had been performed by direct puncture of the common carotid artery<sup>22</sup>. Another milestone in cerebral angiography is the Seldinger puncture technique, described in 1953, giving the possibility to do selective catheterisation of different arteries in the body by one access<sup>23</sup>.

Since then, many developments have been made regarding contrast medium, catheter materials and designs, as well as biplane x-ray systems.

Endovascular treatment of intracranial aneurysms started in the beginning of the 1970's and FA Serbinenko published in 1974 the first attempts to treat aneurysms with balloons<sup>24</sup>. An important device for interventional neuroradiology was the development of Guglielmi detachable coils (GDC), published in 1991, which made the treatment of aneurysms possible with low complication rates<sup>25</sup>.

In 1952, F Bloch from Stanford University and E Purcell from Harvard University were awarded the Nobel Prize for their work on nuclear magnetic resonance, at the time being a chemical analysis. With the introduction of computers the development proceeded and it became possible to use the technique for medical imaging. In 2003, PC Lauterbur and P Mansfield were awarded the Nobel Prize for their discoveries concerning magnetic resonance imaging.

Since 1974, when the first image of a rat was presented, there has been a tremendous advance in MRI, both regarding increasing magnetic field strengths and the evolution of more advanced MR imaging techniques.

As MRA is not using ionizing radiation, it would be a method preferred over CTA, and the technique has been evaluated regarding its capabilities to identify and follow-up aneurysms<sup>18,21,26</sup>. Because MRA requires good cooperation of the patient and takes more time to perform than CTA, it is not the optimal emergency investigation in patients with SAH. However, it has a place in clinical routine for follow-up of coiled aneurysm and in screening for aneurysms in patients with high risk to develop aneurysms.

The development of CT for medical care started during late 1960s and 1971 the first patient was examined. In 1979, G Hounsfield and A Cormack shared the Nobel Prize for the development of computer assisted tomography.

As MR, CT technology has since its beginning undergone an incredible progress from a head scanner with a single scan, taking 5 minutes to perform, to multislice and multi-detector CTs covering the whole body in a scan performed in a few seconds.

Since the beginning of the millennium, the developments in CTA have made it an important tool in the investigation of emergency patients with both ischemic and haemorrhagic stroke including SAH<sup>27,28</sup>.

## Anatomy

### Circle of Willis

The arteries in the circle of Willis consist of an interconnecting arterial polygon and variants are seen from complete circle to hypoplastic or absent parts. It is situated anterior to the diencephalon adjacent to the optic nerves, chiasm and tracts.

A complete circle of Willis (Fig.1) consists of bilateral internal carotid arteries (ICA), reaching the skull through the carotid canals in the skull base and intracranially dividing bilaterally into the anterior cerebral artery (ACA) and middle cerebral artery (MCA). The anterior communicating artery (ACOM) connects the right and left ACA and the ACA segment prior to this junction is named A1 segment and followed by the A2 segment, the latter also called pericallosal artery. The ICAs and their branches are referred to as the anterior brain circulation.

The posterior brain circulation consists of the bilateral vertebral arteries (VA), reaching the skull through the foramen magnum and converging to the basilar artery (BA), which at its top divides into bilateral posterior cerebral arteries (PCA). The connection between posterior and anterior circulation is ensured by a bilateral posterior communicating artery (PCOM) (Fig. 1).

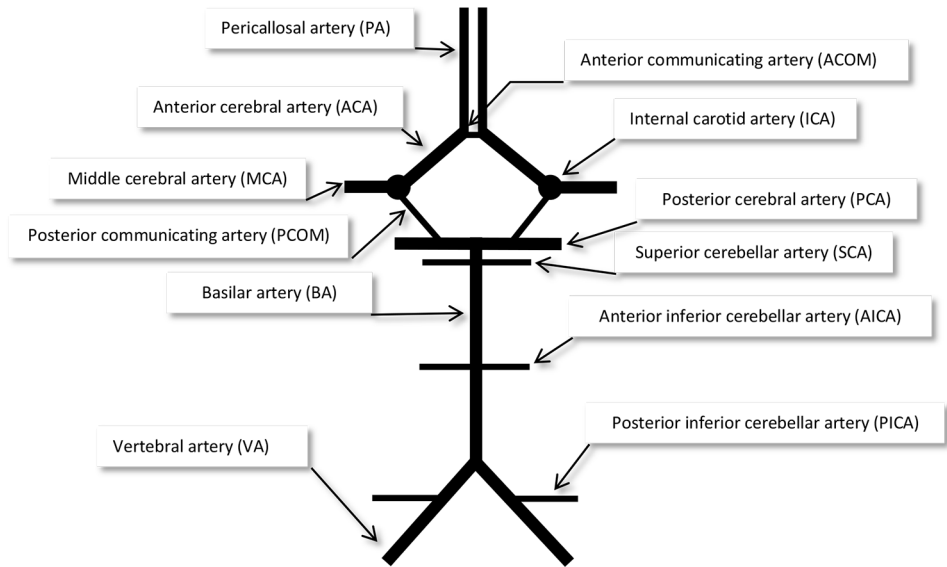


Fig.1 Circle of Willis

From the circle of Willis, the segments of the arteries are named after the origin artery (ACA, MCA, PCA) and numbered with increasing numbers after each division, e.g. A1, A2, M1, M2 or P1, P2 and so forth. The peripheral branches of these arteries are interconnected by a pial arterial network.

In approximately 45-48% of anatomical specimens a complete circle of Willis was seen<sup>29,30</sup>. However, anatomical variations of the circle of Willis occur frequently, consisting of hypoplastic, absent or duplicated parts. The most common anomalies seen are hypoplastic vessels and the most usual site is PCOM (incidence 10-53%), followed by P1 segment (6-18%), A1 segment (2-12%) and ACOM (2-9%). Another anomaly seen in 10-22% is embryonic origin of PCA from the ICA<sup>29</sup>. Multiple anomalies are seen in 7% and the most common is hypoplasia of two vessels for example ACA and PCOM on the same side or PCA on one side and PCOM of the opposite side<sup>30</sup>.

## Imaging methods

### Digital subtraction angiography

DSA is an invasive imaging technique using ionizing radiation to visualize vessels enhanced with iodine-based contrast medium, which are injected after catheterization of a feeding vessel. The subtraction of non-enhanced from enhanced images is used to remove unwanted body structures such as bone from the images. DSA

is performed either on a monoplane or biplane angiographic unit, and both two-dimensional (2D) and three-dimensional (3D) acquisition is possible (Fig.2). An uncomplicated routine DSA confines patients to bed for approximately 1 to 2 hours.

General complication rates have been reported between 0.5-2%<sup>10-12</sup>. However, when DSA is performed by neurointerventional specialists, complication rates as low as 0.3% and 0.06% can be achieved<sup>13,31</sup>.

A complete 2D four-vessel angiography (bilateral ICA and bilateral VA) and 3D angiography has a high sensitivity and specificity to detect intracranial aneurysms and thus it is still the gold standard method for detection of intracranial aneurysms.

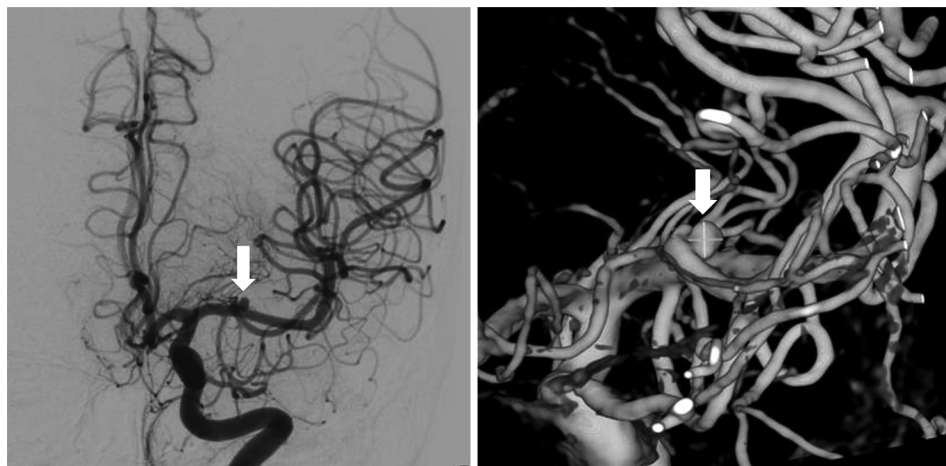


Fig.2 DSA – coronal, 2D (left) and 3D image (right) with contrast medium injection in left ICA, showing a 3 mm aneurysm on left MCA (white arrows).

## Magnetic resonance angiography

MRI is a non-invasive diagnostic imaging technique to investigate the anatomy and function of the body. MRI does not use ionizing radiation as CT and DSA, but strong magnetic fields (generally 1 to 3 Tesla) and radiofrequency waves to form images of the body.

MRA can be performed as contrast-enhanced angiography (CE-MRA) or as a 3D inflow technique, also called time-of-flight MRA (TOF-MRA). In TOF-MRA, the signal from stationary tissue is suppressed while inflowing blood is not, which yields angiograms with the blood in the arteries hyperintense compared to surrounding tissue.

In CE-MRA, the gadolinium-based contrast agent is applied intravenously and influences imaging parameters yielding high signal intensity in the vessels in T1-weighted images. Although acquired as 2D images, these can both in TOF-MRA and CE-MRA be reconstructed and presented as 3D angiograms (Fig.3).

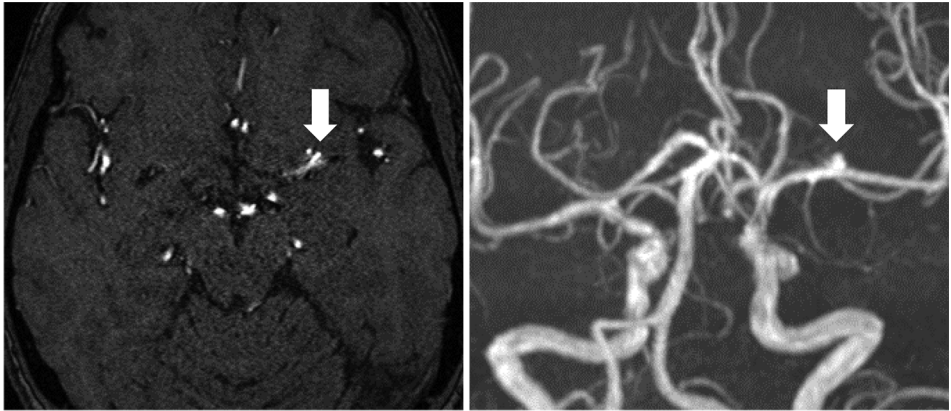


**Fig.3** TOF-MRA at 1.5T – axial projection, 2D source image (left) and 3D maximum intensity projection (MIP)(right) showing a 3 mm aneurysm on left MCA (white arrows).

### Computed tomography angiography

CT is the first line diagnostic imaging technique in many cerebral disorders. In CT and CTA, ionizing radiation is used as in DSA.

CTA is a well-established and fast technique that can be performed as a routine during all hours, which makes it the first-hand imaging technique for patients with SAH diagnosed e.g. on a directly preceding cranial non-enhanced CT. Three-dimensional image processing with maximum intensity projections (MIP) displays the maximum arterial attenuation (measured in HU) in the image i.e. contrast-filled arteries. 2D images and 3D volume-rendering technique as well as MIP are used in CTA (Fig.4).

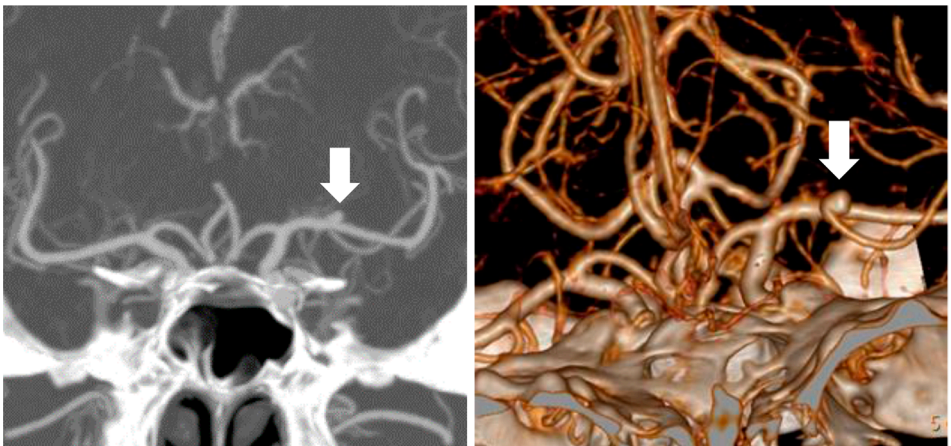


**Fig.4** CTA 2D coronal projection with MIP and a slice thickness 20 mm (left) and 3D volume rendering (right) showing a 3 mm aneurysm on left MCA (white arrows).

## General technical considerations

All imaging modalities have different advantages and disadvantages. One main disadvantage for DSA and CTA compared to MRA is its use of ionizing radiation. Radiation dose in DSA depends on tube voltage (kVp) and tube current (mA) as in CT, however in DSA it also depends on magnification while it in CT depends on the slice scan time (s). In the clinical setting, the goal of DSA and CTA is to produce images of diagnostic quality at lowest possible radiation exposure.

As DSA is an invasive technique with a risk of symptomatic complications it is important to streamline indications for the use of the method and to explore the possible use of other technologies answering the same clinical questions.

Image quality is in all modalities dependent on factors such as image contrast, spatial resolution, image noise and artefacts.

Patient movements in between the two images for subtraction are a well-known source of image artefact in DSA. Image artefacts in CT are usually shading artefacts, ring artefacts or streak artefacts. The most common shading artefacts are beam-hardening, due to imperfect correction. Others are partial volume effects and scatters. Ring artefacts are caused by detector inaccuracies. Metal and motion of the subject causes streak artefacts.

Inappropriate contrast injection timing might cause a problem for DSA, CTA and CE-MRA alike, but not TOF-MRA, leading either to disturbing vein filling when investigating arteries or incomplete artery enhancement related to too early timing. Knowledge of the patient's renal function is important, since administration of iodine-based and gadolinium-based contrast medium may worsen renal insufficiency.

Aneurysms treated with microsurgical clips or endovascular coils imply extra challenges for the different modalities as they in CT may cause beam hardening artefacts and in MRA susceptibility artefacts. MR artefacts from coils may increase with higher field strength, however, this is MR parameter dependent and for example the use of higher bandwidth and shorter TE at 3T may yield smaller metal artefacts than on 1.5T.

## Pathology

### Aneurysms

An aneurysm is defined as a persistent dilatation of the arterial wall. The intracranial arterial wall consists of adventitia (outer loose connective tissue), media (muscular layer) and intima (inner layer with elastic lamina and endothelial layer)<sup>32,33</sup>. Intracranial arteries differ from other similar sized arteries by the adventitia and



media being considerably thinner. The prevalence of aneurysms in autopsy studies is approximately 2%<sup>1</sup>.

The risk of unruptured aneurysms to rupture depends on multiple factors such as location and size of the aneurysm and to clinical factors as age, gender, smoking, hereditary diseases and previous SAH in patients with multiple aneurysms. The overall rupture risk is between 1-2%<sup>34</sup>.

They are often located in arterial bifurcation (saccular) or can represent a fusiform dilatation of the arterial wall (non-saccular).

Saccular aneurysms (Fig.5) originate usually from a localized defect in the muscular and elastic layers in the arterial wall of the parent artery and the aneurysmal pouch is formed by the intimal layer and the adventitia. The size of an aneurysm may range from small <10mm to large 11-24 mm and giant >25mm. Most saccular aneurysms have an unknown aetiology, although increased incidence is seen in hereditary diseases as polycystic kidney disease and inherited vascular conditions as Marfan syndrome. Multiple aneurysms are detected in 8-34% of cases<sup>35-37</sup>.

A correlation is seen between variations of Circle of Willis and aneurysms especially regarding asymmetric ACA and PCOM<sup>38</sup>.

Non-saccular or fusiform aneurysms (Fig.6) involve the entire arterial wall and are less common but usually aetiology such as dissection, trauma, infection or flow-related factors can be identified.

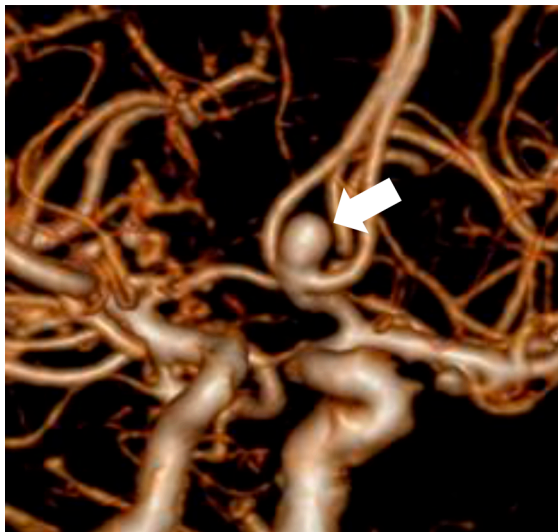


**Fig.5** Saccular aneurysm (white arrow) on ACOM, size 7 mm, displayed on 3D CTA.





Fig.6 Fusiform aneurysm (arrows) on a M3-segment of the MCA visualized on DSA – oblique frontal 2D view (left) and 3D view (right).

### Cerebral vascular malformations

Arteriovenous malformations (AVM) are divided into three different types – pial, dural and mixed pial-dural.

Pial or parenchymal AVM consist of dilated arteries, collecting into a nidus without a capillary bed and draining into veins. On the feeding artery or intranidal, flow-related aneurysms are seen in 10-18%<sup>39</sup> (Fig.7 and Fig.8).

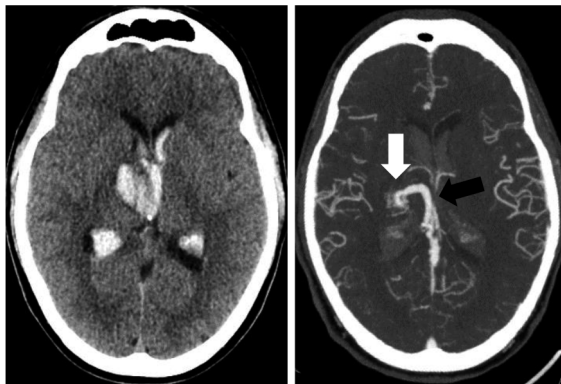
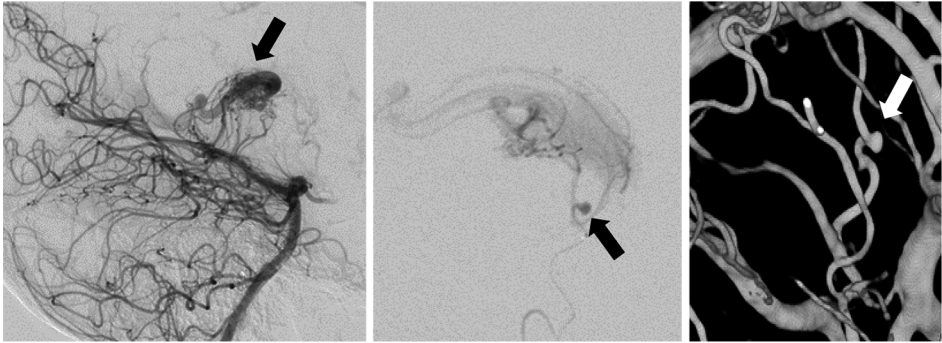
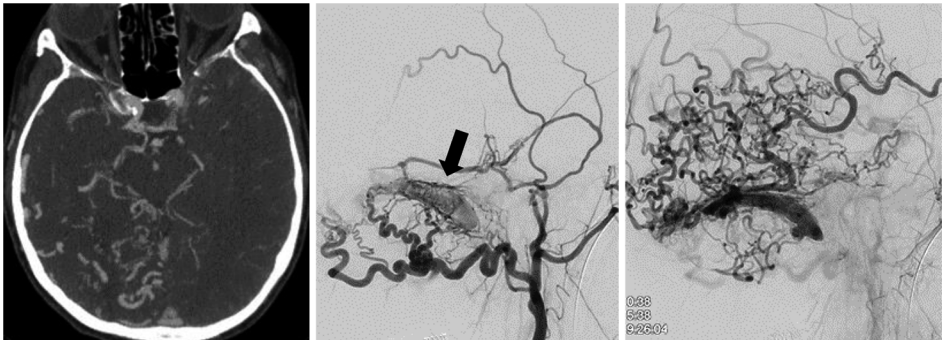


Fig.7 Patient with an intraparenchymal hematoma right thalamus with intraventricular haemorrhage shown on non-enhanced CT, axial view (left); CTA, axial view, shows a small AVM (white arrow) with a draining vein (black arrow) (right).



**Fig.8** Same patient as in Fig.7, DSA, lateral view, shows the AVM (black arrow) (left); DSA, enlarged lateral view, superselective injection, shows a small feeder aneurysm (black arrow) (middle); DSA, 3D, shows the small aneurysm (white arrow) (right).

Dural AVM, often described as dural arteriovenous fistula (dAVF), consist of dilated meningeal arteries and a network of micro fistulae draining into dural sinus (Fig.9). Mixed pial-dural AVM consist of parenchymal AVM, with arterial supply from intracranial arteries as well as dural arteries.



**Fig.9** CTA axial view, showing multiple dilated veins in the right hemisphere (left); DSA lateral view, arterial phase, showing early filling of transverse sinus (black arrow) (middle); DSA lateral view, venous phase, showing dilated veins as in cortical hypertension (right).

Other vascular malformations are cavernoma, being clustered dilated endothelial lined channels (Fig.10); capillary telangiectasia, consisting of clustered dilated capillaries; or development venous anomaly (DVA) which consists of thickened veins.

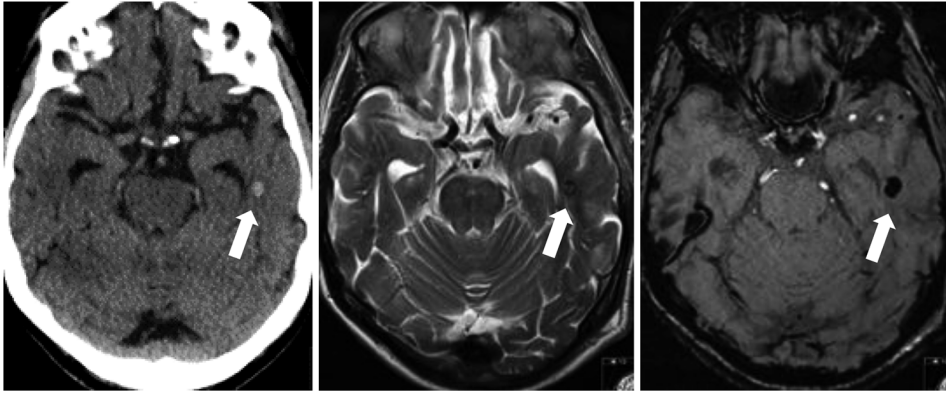


**Fig.10** Cavernoma (white arrows), left temporal lobe, shown at non-enhanced CT, axial view (left); T2-weighted MR, axial view (middle); susceptibility weighted MR (sensitive to haemorrhage), axial view (right).

### Other vascular diseases of the brain

Ischemic stroke is either a thromboembolic disease caused by large artery atherosclerosis, cardioembolism (Fig.11) or small vessel occlusion (lacune).

Non-infectious vasculitis is either granulomatous as for example neurosarcoidosis or without known cause, as primary angiitis<sup>40</sup>. It can also be associated with collagen vascular diseases such as systemic lupus erythematosus or drug-related e.g. in conjunction with amphetamine abuse.

Infectious vasculitis is associated with diseases as for example syphilis, tuberculosis and human immunodeficiency virus (HIV).

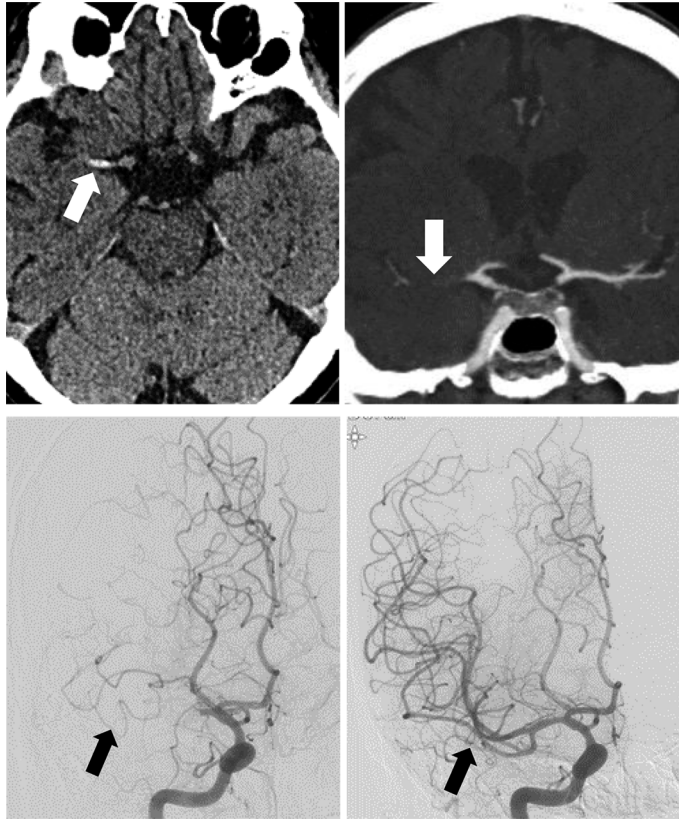


**Fig.11** Patient with atrial fibrillation and neurological symptoms from right hemisphere, where non-enhanced CT, axial view, shows the embolus (white arrow) as dense vessel sign (left upper); CTA, coronal view, showing occluded M1-segment, MCA right side (white arrow) (right upper); DSA, frontal view, which confirms CTA findings of occluded M1-segment (black arrow) (lower left); DSA, frontal view, showing a recanalized right MCA (black arrow) after thrombectomy (right).

Other vascular disorders are fibromuscular dysplasia, with fibrous and muscular thickening of the arterial wall, probably caused by hyperplasia of the media, alternating with dilatation of the wall, caused by thinning of the media. It involves primarily cervicocephalic arteries and more seldom intracranial arteries (Fig.12)<sup>41</sup>.

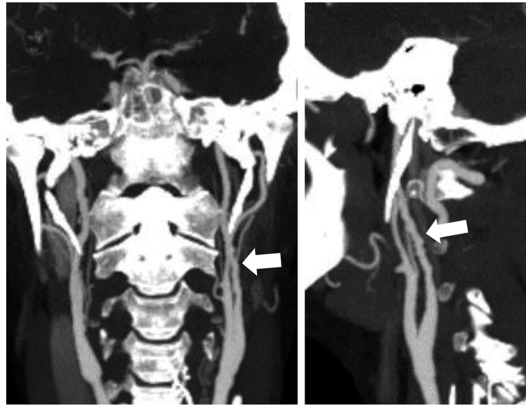


Fig.12 Fibromuscular dysplasia, bilaterally ICA (white arrows), CTA coronal view (left) and sagittal view, left ICA (right).

Moyamoya is a chronic, occlusive cerebrovascular disease involving bilateral stenosis or occlusion of the terminal portion of the ICAs and/or the proximal portions of the ACAs and MCAs. It results in an extensive collateral network giving an appearance of a “puff of smoke” on DSA, in Japanese moyamoya<sup>42</sup>(Fig.13).

Hematologic diseases such as sickle cell disease may give a cerebrovascular occlusive vasculitis, probably related to stasis and ischemia in the vasa vasorum in ICAs and proximal ACAs and MCAs.

Reversible cerebral vasoconstrictor syndrome (RCVS) is characterized by the association of severe headache and cerebral angiography giving an appearance of “string and beads”. It is sometimes combined with cortical SAH<sup>43</sup> (Fig.14).



Fig.13 Moyamoya disease, shows stenosis of left MCA (white arrows) TOF-MRA source image, axial view (left), TOF-MRA, MIP (middle) and DSA, frontal view (right).



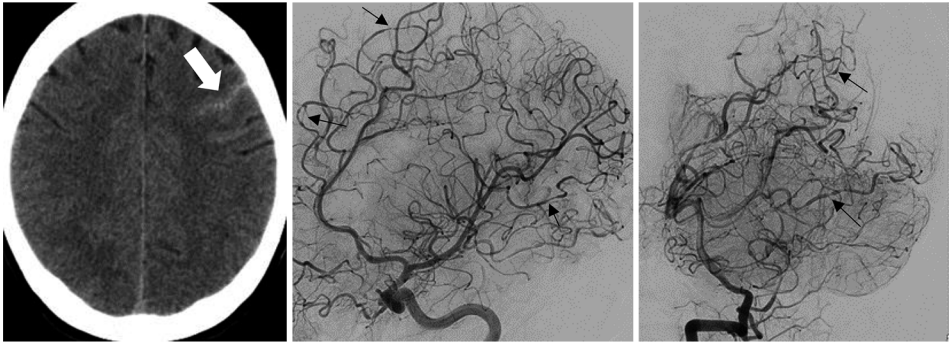


**Fig.14** Small cortical SAH (white arrow) on non-enhanced CT (left); DSA, oblique view, shows “strings and beads” in reversible cerebral vasoconstriction syndrome (black arrows), distal branches of ACA and MCA (middle) and PCA (right).

Angiographic methods including DSA, CTA and MRA, as well as CT and MR, are used in order to be able to diagnose vascular cerebral diseases. Different methods may be used depending on the specific clinical question or diagnosis as illustrated above. Selecting the right imaging method and arriving at a correct diagnosis is a prerequisite for treatment decisions, irrespective whether the treatment might involve surgery, endovascular or medical treatment.

## Subarachnoid haemorrhage

Subarachnoid haemorrhages are divided into traumatic and non-traumatic SAH. In the latter group approximately 85% are caused by aneurysms.

The classic presentation of an aneurysm rupture is sudden headache, nuchal rigidity, nausea, vomiting and loss of consciousness, where the level of consciousness often improves slowly. Also focal neurological signs can appear especially from cranial nerves III-IV due to mass effect.

The diagnosis of SAH is made by non-enhanced CT or lumbar puncture. The appearance of SAH (Fig.15) on non-enhanced CT is classified according to Fisher<sup>44</sup> (Table 1).

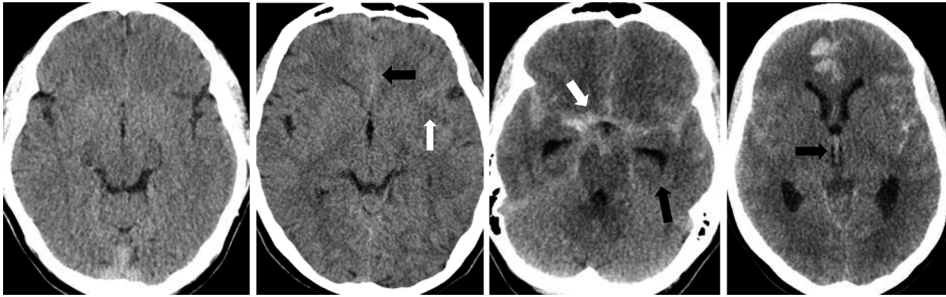


**Fig.15** The 4 Fisher grades illustrated in different patients. Fisher grade 1: no SAH (outer left); Fisher grade 2: SAH in the anterior interhemispheric fissure (black arrow) and left sylvian fissure (white arrow) (middle left); Fisher grade 3: SAH in the basal cistern (white arrow), bilateral sylvian fissures and the anterior interhemispheric fissure. Also prominent temporal horns of the lateral ventricles (black arrow) are seen due to hydrocephalus (middle right); Fisher grade 4: intraventricular haemorrhage, in the third ventricle (black arrow) as well as left posterior horn of the lateral ventricle, and SAH in both sylvian fissure and anterior interhemispheric fissure (outer right).

**Table 1.** Fisher grading of subarachnoid haemorrhage (SAH) on non-enhanced CT.

Fisher grading	Image appearance
Grade 1	No haemorrhage
Grade 2	Diffuse deposition or thin layer of blood less than 1 mm
Grade 3	Localized clot and/or layer over 1 mm
Grade 4	Intracerebral or intraventricular blood with diffuse SAH

According to the pattern of haemorrhage, it is in many cases possible to appreciate the location of the aneurysm (Fig.16)<sup>45</sup> and which of the aneurysms has ruptured, if multiple aneurysms are found. The incidence of multiple aneurysms in SAH patients is between 12-45%<sup>36,37,46,47</sup>.

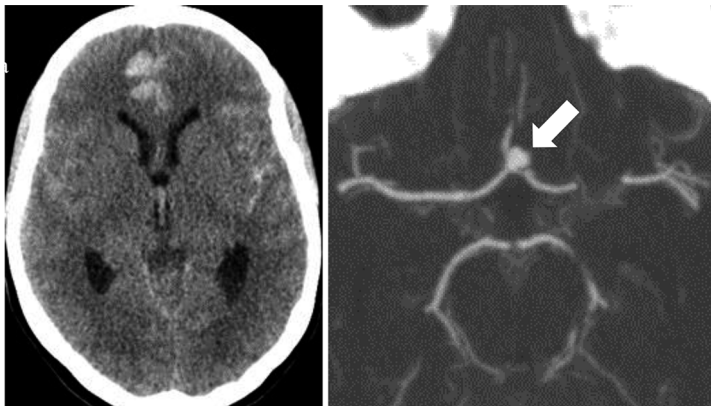


**Fig.16** Non-enhanced CT with Fisher grade 4, shows SAH in the anterior interhemispheric fissure and small right frontal intraparenchymal haemorrhage as well as SAH bilaterally sylvian fissure and intraventricular haemorrhage in third ventricle (left); CTA, in the same patient, showing an ACOM aneurysm (white arrow) (right).

A sub-group with a specific pattern of haemorrhage, defined to the cisterns around the midbrain, is called perimesencephalic SAH and these are seldom caused by aneurysms (Fig.17). The patient's symptoms tend to be more benign than patients with a ruptured aneurysm. Rebleeding is not seen and usually patients with a perimesencephalic pattern of SAH, have a favourable outcome.<sup>93</sup>



Fig.17 Non-enhanced CT, axial projection with perimesencephalic pattern of SAH.

## Treatment of intracranial aneurysms

The goal of aneurysm treatment is to prevent bleeding or rebleeding. Major therapeutic alternatives are microsurgical clipping and endovascular treatment with coils (Fig.18).

Endovascular treatment consists of superselective catheterization of the aneurysmal pouch and its obliteration with coils. Different approaches may be used as remodelling technique with temporary balloon occlusion of parent artery. When the aneurysmal neck is very wide, stent placement in the adjacent artery may even be necessary together with coiling. Parent artery occlusion can also be an option mainly in ICA and VA. The most recent devices developed are flow-diverters and intrasaccular flow disrupters.



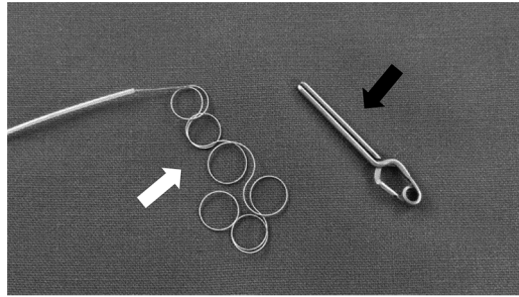


**Fig.18** Endovascular coil (white arrow) and a microsurgical clip (black arrow).

After endovascular treatment, a follow-up angiographic examination is important because of the risk of recanalization in aneurysms treated with endovascular coils<sup>48,49</sup>. Reasons for recanalization of coiled aneurysms are coil compaction due to arterial flow in combination with the resorption of the thrombus in the aneurysm or a blood clot in the subarachnoid space (Fig.19), ongoing growth of the aneurysm due to the initial disease in the arterial wall or a combination of coil compaction and regrowth of the aneurysm.

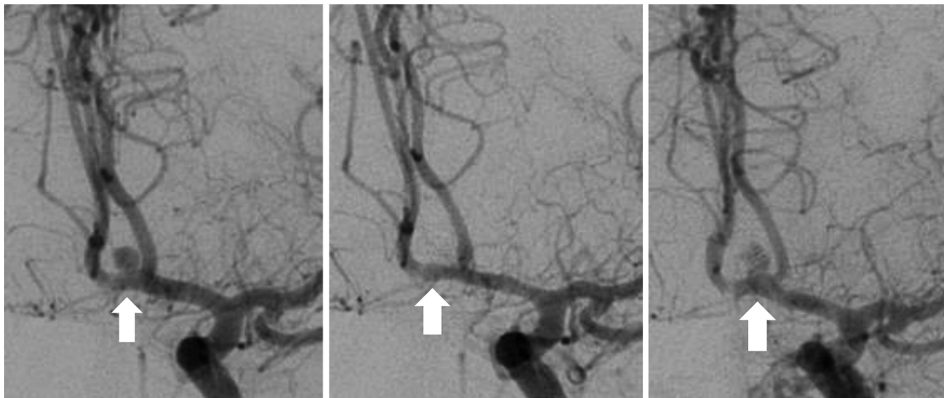


**Fig.19** DSA, all oblique view, aneurysm at ACOM (white arrow) (left); occluded aneurysm after treatment with coils (white arrow) (middle); partial recanalization after 15 months (white arrow) (right). (*Paper I, Fig.2, reprinted with permission*)

When a patient has been successfully treated with clipping, no angiographic control is usually performed. If necessary CTA is an option for follow-up, since the clip usually is small and consists of titan or titan alloy, giving very little metal artefacts on CT.

If endovascular treatment with coils is used, CTA is not appropriate due to beam hardening artefacts from platinum coils. The artefacts from the coil mesh do, however, not disturb the evaluation with MRA.

When treatments are performed with only stents and flow-diverters in the artery, CTA is adequate and MRA is not the best option, because of metal artefacts from nitinol and cobalt chromium.

A combination of microsurgical clipping and endovascular coiling may be used if the aneurysm is not possible to occlude with only one of the methods (Fig.20). It may be difficult to decide which angiographic method, except DSA, is best to use to assess the grade of occlusion of these aneurysms.

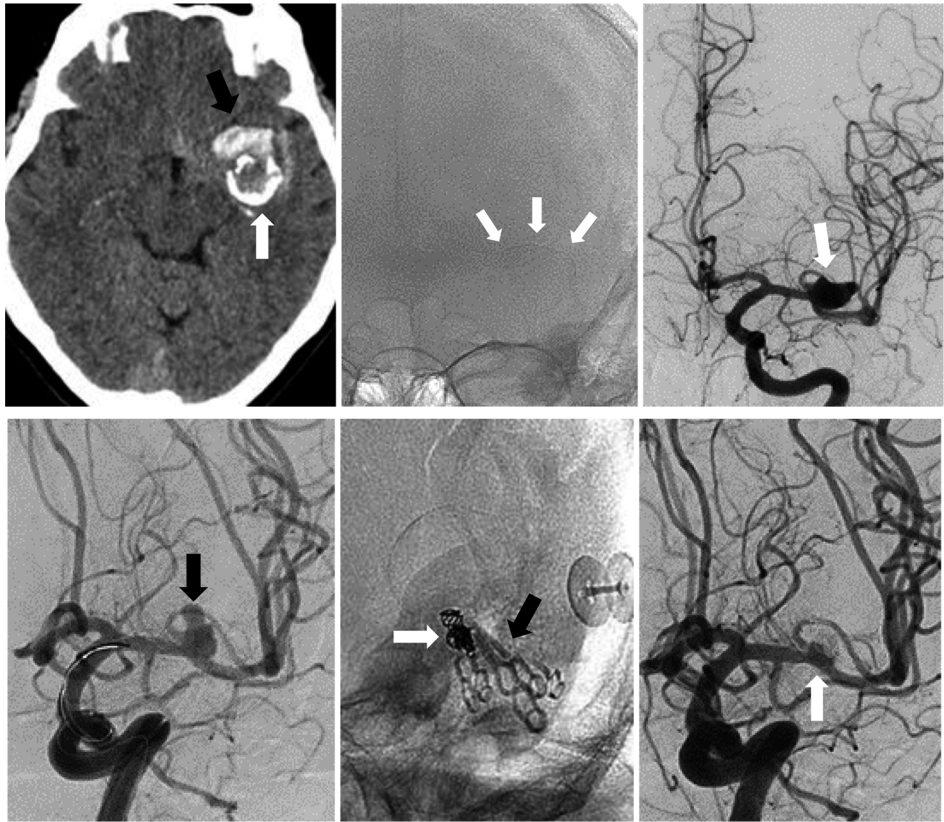


**Fig.20** Non-enhanced CT, axial view, shows SAH (black arrow) and calcifications (white arrow) seen in the aneurysmal wall (upper left); Non-subtracted DSA, frontal image, showing the faint calcification (white arrows) (upper middle); DSA, frontal view, showing the broad neck aneurysm in the MCA bifurcation (white arrow) (upper right); DSA, oblique view, aneurysm remnant (black arrow) after operation (lower left); non-subtracted DSA, oblique view, shows the clips (black arrow) and coils (white arrow) after endovascular treatment (lower middle); DSA, oblique view, after treatment (white arrow) with clips and coils (lower right).

Microsurgical clipping after recanalization of an aneurysm treated by endovascular coiling is an option to retreat the patient if a retreatment with endovascular technique is difficult or the risk of new recanalization is assessed as high. To get an opti-

mal position of the clip, the aneurysm neck has to be free of coil loops otherwise it might be difficult to occlude the aneurysm with a microsurgical clip (Fig.21).

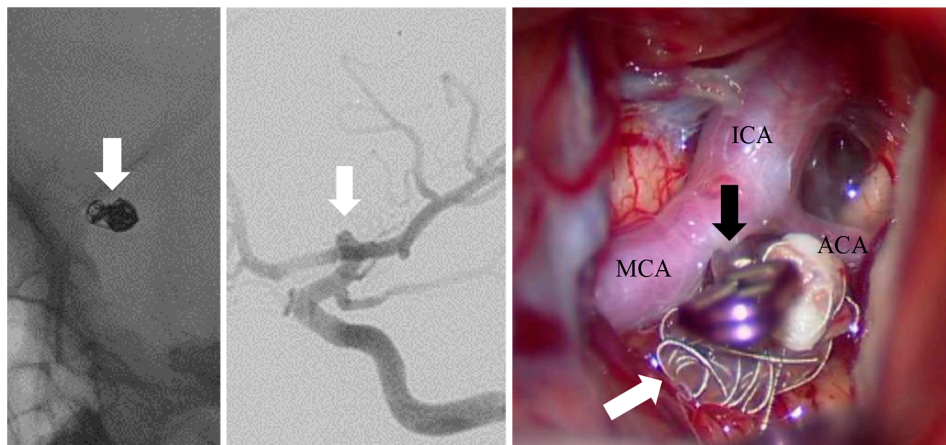


Fig.21 Follow-up DSA, oblique view, non-subtracted image of coils (white arrow) (left) and subtracted image with a recanalization of the aneurysm neck at the top of the ICA (white arrow) (middle); Microscopic view during operation of the recanalized aneurysm (coils – white arrow) at the top of the ICA and the microsurgical clip (black arrow) placed at the revascularization at the base of the aneurysm (the arteries involved are displayed) (right).

## Background for study initiation

### Paper I

Since the mid-1990s, neurointerventional treatments are performed in Lund on a regular basis concerning aneurysms as well as other vascular malformations and diseases. Patients treated for an aneurysm with coiling have to be controlled with angiography due to the risk of recanalization and bleeding. At the beginning, DSA was the only reliable follow-up method.

Around 2000, the technique of MRA for follow-up of coiled aneurysms compared to DSA as gold standard was evaluated in several studies. Studies focused on MR field strengths and MRA methods such as TOF-MRA at 1T<sup>50</sup> and at 1.5T<sup>51,52</sup>, CE-MRA<sup>53</sup>, contrast enhanced and non-enhanced TOF-MRA<sup>54</sup> and TOF-MRA compared with CE-MRA<sup>55</sup>. When 3T MR scanners were available, a comparison of TOF-MRA at 3T and 1.5T was presented<sup>56</sup>. All studies consented in the usefulness of MRA for the evaluation of coiled aneurysms.

We decided to perform a study (Paper I) evaluating the parameters field strength (1.5 and 3T) and MRA technique (TOF-MRA and CE-MRA) for follow-up of coiled aneurysms with DSA as gold standard.

## Paper II

The rapid development of multislice CT scanners and CTA techniques in the beginning of the 21st century made it possible to use CTA of intracranial arteries as the first method of choice in emergency patients with SAH. A study presented in 2004<sup>57</sup> concluded that high tube voltage was superior concerning image quality and vessel delineation, although discussions had earlier been favouring low tube voltage. Therefore, we investigated whether low (90 kVp) or high (120 kVp) tube voltage was optimal concerning image quality.

A further aim of Paper II was to evaluate the impact of an increase of iodine concentration in contrast medium from 300 to 400 mgI/ml on arterial attenuation and thereby image quality.

## Paper III

Fast and accurate detection of aneurysms, especially in patients with SAH, is important prior to treatment decisions and regarding decreasing the risk of rebleeding. CTA was early identified as diagnostic method in patients with SAH<sup>58</sup> and later as a reliable method using 4- to 16-slice CTs<sup>59</sup>. As CT development had advanced it could be argued that more advanced multislice techniques (16- to 128-slice CTs) could improve image quality and thereby diagnostic accuracy even more, and that this might further ensure pretreatment decisions to be based on CTA and not on DSA, the gold standard.

Therefore, we sought to evaluate diagnostic accuracy of CTA and arterial attenuation of intracranial arteries as an image quality parameter in patients with non-traumatic SAH based on the results in Paper II. The latter had not been investigated before.



# Aims

## Paper I

- To compare the agreement between TOF-MRA and CE-MRA at 3T and TOF-MRA at 1.5T with DSA for the follow-up of intracranial aneurysms treated with detachable coils in order to select the best MRA method for treatment follow-up.

## Paper II

- To evaluate the impact of an increase of iodine concentration in contrast medium from 300 to 400 mgI/ml and the effect of decreased tube voltage from 120 to 90 kVp on image quality and arterial attenuation in CTA of intracranial arteries.

## Paper III

- To evaluate the diagnostic accuracy of CTA in non-traumatic SAH compared to DSA and to assess the arterial attenuation (HU) as an image quality factor in this aspect.



# Methods

## Ethics

All studies were approved by the regional research-ethical committee (LU 981-03, Dnr 2011/702 and Dnr 2012/273). For Paper I, all subjects gave written informed consent. Written informed consent was waived by the ethical committee for Papers II and III.

## DSA technique

DSA was performed on a biplane angiography unit, Integris (Paper I and III), Allura Xper FD20/10 (Paper III) or a monoplane unit, Allura Xper FD20 (Paper III) (all Philips Healthcare, Best, The Netherlands).

The contrast medium iohexol 240 mgI/ml (Omnipaque®; GE Healthcare, Chalfont St. Giles, UK) was used for Paper I and III.

Images were acquired in at least 4 standard projections for each artery in 2D acquisition and in Paper III also 3D acquisition was performed in approximately 60% of patients.

DSA was used as gold standard in Paper I and III.

## MRA technique

MRA examinations in Paper I were performed on a 1.5T Intera and a 3T Intera MR scanner (Philips Healthcare, Best, The Netherlands).

For CE-MRA, a test injection of 2 ml gadolinium-based contrast medium (Magnevist®, Schering AG, Germany), was followed by 30 ml saline at 2 ml/s. The contrast bolus of 18 ml was injected, followed by 30 ml saline with the same injection rate.

MR parameters are shown in Table 2.



Table 2. MR parameters

	3T TOF-MRA	1.5T TOF-MRA	3T CE-MRA
Sense ( <i>P</i> reduction)	2.00	1.50	1.40
No of slices	100	100	100
Slice thickness (mm)	0.50	0.50	0.50
TE (ms)	3.5	6.9	2.0
TR (ms)	26	25	5.8
Total scan duration (min)	5:58	7:38	0:49
Measured voxel size (mm)	0.39 x 0.68 x 1.00	0.46 x 0.46 x 1.00	0.68 x 0.76 x 1.00
Reconstructed voxel size (mm)	0.24 x 0.24 x 0.50	0.45 x 0.45 x 0.50	0.49 x 0.49 x 0.50
Band-width (Hz)	217.1	108.6	452.9
Matrix scan	640 x 367	496 x 496	368 x 329
FOV (mm)	250	230	250
Flip angle (°)	20	20	30

## CTA technique

CTA was performed in Paper II on a Philips MX 8000 IDT 16-slice CT. This CT was also used in Paper III as well as the other CTs at our department including Brilliance, 40-slice and 64-slice, and iCT 128-slice (all Philips Healthcare, Best, The Netherlands). The area examined covered the level of the fifth cervical vertebra to the vertex of the skull.

A contrast medium bolus of 80 ml (Paper II) and 80 to 105 ml depending on scan duration (Paper III) was injected by a power injector (Medrad Inc., Warrendale, PA, USA) at an injection rate of 5 ml/s, followed by an injection of 40 ml saline at the same rate. Prior to main injection, a standardized test bolus scan was performed to determinate each patient's individual scan delay.

In Paper II, patients were consecutively assigned to one of three protocol groups displayed in Table 3.

Table 3. Number of patients in Paper II in the three different groups.

	Group I	Group II	Group III
Contrast concentration, mgI/ml	300	400	400
Tube voltage, kV	120	120	90
Tube current, mAs	229	229	564
CTDI <sub>vol</sub> , mGy	32.6	32.6	36.8
Patients (number)	15	15	33

In Paper III, being a retrospective study in a clinical setting, the iodine concentration was 300 mgI/ml, 350 mgI/ml or 400 mgI/ml, depending on the contrast medium used at the time. A standardized protocol was used and the original slice

thickness was 0.8 mm. The tube voltage varied between 80-120 kVp and tube current between 229 – 745 mAs.  $CTDI_{vol}$  was between 23.5 – 36.8 mGy.

## Study groups and main methods

In Paper I, 37 patients with 41 aneurysms treated with endovascular coils were prospectively and consecutively included during one year from April 2004. All patients were included prior to a scheduled follow-up DSA. Additional MRA examinations (Table 2) were performed within one day, except for three patients with delayed DSA examinations due to emergency patients blocking the angio suite. With DSA as gold standard, the different MRA examinations were evaluated for recanalization of coiled aneurysms.

For Paper II, 63 consecutive patients were included during 2005-2006, all referred to the Section of Neuroradiology for clinical CTA of intracranial arteries. Three consecutive protocol groups were selected according to Table 3. On the different CTA examinations, means of arterial attenuation and also grading of image quality were performed.

Paper III included retrospectively 326 consecutive patients with non-traumatic SAH between the years 2005-2011, undergoing CTA and DSA at our hospital within 7 days of each other. With DSA as gold standard, the different CTA examinations were evaluated for diagnostic accuracy and also image quality by measurements of arterial attenuation in ICA.

## Data evaluation

### Paper I

In Paper I, three neuroradiologists evaluated MRA and DSA images on a View Forum workstation (Philips Healthcare, Best, The Netherlands) using source images, MIP, MPR and VR reconstructions. Comparable to the clinical setting, observers were allowed to alter thickness and angulation on MRA images and also to see the pre- and post-treatment DSA. Different MRA sequences were evaluated separately and with at least one week in between. First all assessments were done individually for all MRA and DSA examinations and secondly consensus was reached in all cases showing disagreement. The following main data were extracted during the evaluation process:

- Classification of aneurysms concerning recanalization on DSA and MRA according to the modified Raymond classification (Fig.22)

- Classification of the aneurysm on DSA and MRA as being at risk for rebleeding and therefore patients being candidates for discussion of retreatment (yes or no)
- Assessment of regrowth of aneurysms on DSA and MRA, defined as >20% enlargement of the recanalized aneurysm and coil mesh compared with the initial size of the aneurysm prior to treatment (amount of regrowth)
- Assessment of presence of aneurysm recanalization (no, minor, major)
- Size of susceptibility artefacts from the coil mesh on MRA
- Evaluation of visualization of parent artery on MRA (yes or no)
- Rating of image quality as good or poor for MRA

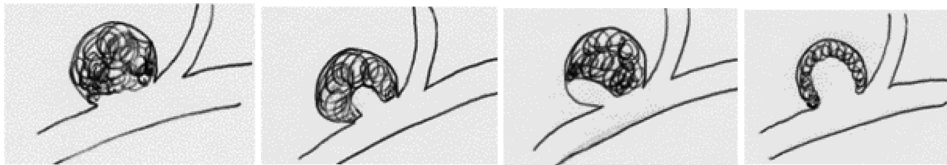


Fig. 22 Recanalization according to a modified Raymond classification: 0 = complete occlusion (not illustrated) 1 = minor recanalization, at the base of the aneurysm (outer left) 2a = moderate central recanalization (middle left) 2b = moderate excentric recanalization (middle right) 3 = major recanalization (outer right) (*Paper I, Fig.4 reprinted with permission*)

## Paper II

In Paper II, two neuroradiologists graded image quality on a dedicated workstation (Extended Brilliance Workspace, Philips Healthcare, Best, The Netherlands) displaying source images and MIP and VR were reconstructed. Cases were presented in a random order without any technical information. Grading of image quality was performed in consensus. The following main data were extracted during the evaluation process:

- Arterial enhancement (HU) measured bilaterally in the ICA, M1-segment and M2-segment and also in the white matter above the lateral ventricle as an indicator of noise
- Reconstruction of 5 mm axial MIP slices and selecting appropriate window level and width for best artery depiction
- MIP and VR for image quality grading
  - Assessment of artery definition concerning M1- and M2-segments on MIP and M2-segments on VR, using a four-graded scale where grade 1 represents a

non-diagnostic artery definition and grade 4 represents excellent artery definition

- Assessment of general impression on VR, using a four-graded scale where grade 1 represents non-diagnostic image quality and flying pixels disturbing artery assessment and grade 4 represents excellent image quality, no flying pixels
- Definition of a cut-off level of arterial attenuation (HU) in ICA above which at least 90% of the examinations should have standard or excellent image quality
- CTDI<sub>vol</sub> measurements and average eye lens dose calculation with a phantom

### Paper III

- In Paper III, evaluations were performed in PACS and RIS (Sectra AB, Linköping, Sweden) by one neuroradiologist. All non-enhanced CT were reviewed and parameters were extracted from this review as well as the reports of DSA and CTA including the clinical records. The following main data were extracted during the evaluation process:
- Detectability, localization and largest diameter of aneurysms with DSA as well as classification of aneurysms as ruptured or non-ruptured
- Classification of aneurysms per patient, per aneurysm and per ruptured aneurysm, as true positive, false positive or false negative on CTA as well as secondary detectability of false negative aneurysms for CTA
- Qualification of the reporting neuroradiologist (non-interventional or interventional)
- Image quality of CTA by means of arterial attenuation (HU)
- Fisher grading scale of SAH and definition of a subgroup of perimesencephalic SAH

## Statistical analysis

### Paper I

- Range of agreement by  $\kappa$  analysis
- Comparison of coil artefacts was evaluated with Wilcoxon signed rank test

## Paper II

- Welch two sample t-test for group differences for measurements of arterial attenuation (HU) with significance level of  $p \leq 0.05$
- Wilcoxon rank sum test for image quality grading
- Scatter plot for visualization of the correlation between arterial attenuation in ICA and window width

## Paper III

- Four-field table data on diagnostic agreement per patient, per aneurysm and per ruptured aneurysm
- Exact binominal tests to calculate sensitivity, specificity, accuracy, positive and negative predictive value, including 95% confidence intervals (CI) for detection of aneurysms
- One-way analysis of variance of arterial attenuation (HU) to compare false-negative aneurysms with true-positive and true-negative ruptured aneurysms
- Logistic regression analysis between aneurysm size and arterial attenuation, assessing the probability to detect an aneurysm if arterial attenuation is either  $< 340$  or  $\geq 340$  HU

# Results

## Paper I

Distribution of the grade of recanalization on DSA according to the modified Raymond classification used is shown in Table 4.

Statistical analysis with comparison of agreement with DSA in the total material showed moderate agreement for TOF-MRA at 3T ( $\kappa=0.43$ ), fair agreement for TOF-MRA at 1.5T fair ( $\kappa=0.21$ ) and poor agreement for CE-MRA at 3T ( $\kappa=0.17$ ).

The classification was divided into two groups aiming at separating no (0) or minor recanalization (1, 2a) from major recanalization (2b, 3), the latter requiring consideration of retreatment. Statistical analysis showed moderate agreement with DSA for TOF-MRA at 3T and 1.5T as well as CE-MRA 3T ( $\kappa=0.50$ ,  $\kappa=0.42$  and  $\kappa=0.40$  respectively). The sensitivity and specificity for any recanalization as well as major recanalization are displayed in Table 5.

Regrowth was seen on DSA in eight patients, but only four of them were detected with TOF-MRA at 3T and 1.5T and three of them with CE-MRA at 3T.

Endovascular retreatment had been performed in nine patients with major recanalization; six of them had aneurysm regrowth.

**Table 4.** Classification and number of coiled aneurysms according to DSA.

Grade	0	1	2a	2b	3
Aneurysms	6	5	4	17	9

**Table 5.** Sensitivity and specificity with regard to any and major recanalization (95% confidence interval). Number of patients (n) on DSA.

		3T TOF-MRA	1.5T TOF-MRA	3T CE-MRA
Any recanalization (n=35)	sensitivity	91.4% (82.8-99.9)	88.6% (78.9-98.3)	82.8% (71.2-94.4)
	specificity	94.6% (87.7-100)	89.7% (80.4-99.0)	89.7% (80.4-99.0)
Major recanalization (n=26)	sensitivity	57.7% (41.8-72.2)	50.0% (34.7-65.3)	61.5% (46.1-75.9)
	specificity	100%	100%	80.0% (67.8-92.2)

Susceptibility artefacts from the coil mesh were significantly larger on TOF-MRA at 1.5T than at 3T ( $p=0.002-0.007$ ) and CE-MRA at 3T ( $p<0.001$ ).

The parent artery was not visualized due to coil artefacts on TOF-MRA in one examination at 3T, in one at 1.5T and two at CE-MRA 3T, by two of the observers although one observer identified all parent arteries.

The image quality in TOF-MRA was rated as good in all examinations at 1.5T, but at 3T, one observer considered the image quality poor in one examination. In CE-MRA 3T, all observers had marked the same three examinations as poor, but also additional 7, 6 and 2 examinations were graded as poor by the three observers, respectively.

## Paper II

Higher iodine concentration in contrast medium, rendered significantly higher mean arterial attenuation (Table 6) in the ICA (Group I vs. II;  $p=0.03$ ) and a similar trend was seen for M1 and M2 segments although not statistically significant.

In Group III, including examinations with lower tube voltage (90 kVp), the arterial attenuation increased significantly in ICA, M1 and M2 segments (Group II vs. III;  $p<0.01$ ).

An increase of iodine concentration from 300 to 400 mgI/ml (Group I vs. II) resulted in a mean increase of arterial attenuation in the ICA of 18%. A reduction of tube voltage from 120 to 90 kVp (Group II vs. III) at iodine concentration of 400 mgI/ml resulted in an increase of mean arterial attenuation in the ICA of 37%. The combined effect of both parameters (Group I vs. III) resulted in an increase of 61%.

**Table 6.** Arterial attenuation (mean HU  $\pm$  SD).

	Mean HU $\pm$ SD		
	Group I (300/120)	Group II (400/120)	Group III (400/90)
ICA	360 $\pm$ 75	424 $\pm$ 82	579 $\pm$ 157
M1	333 $\pm$ 68	382 $\pm$ 84*	525 $\pm$ 133
M2	306 $\pm$ 66	354 $\pm$ 82*	465 $\pm$ 127

\*One patient was excluded from measurements due to aneurysm coil artefacts

No statistically significant difference was seen for mean SD of attenuation (HU) in the white matter (Group I 13.76  $\pm$  2.06; Group II 13.75  $\pm$  1.30; Group III 14.1  $\pm$  1.81).

Plotting the window width chosen during the image quality evaluation procedure, against the mean arterial attenuation in the ICA showed a clear tendency of broader window settings with increased HU (Fig.23).

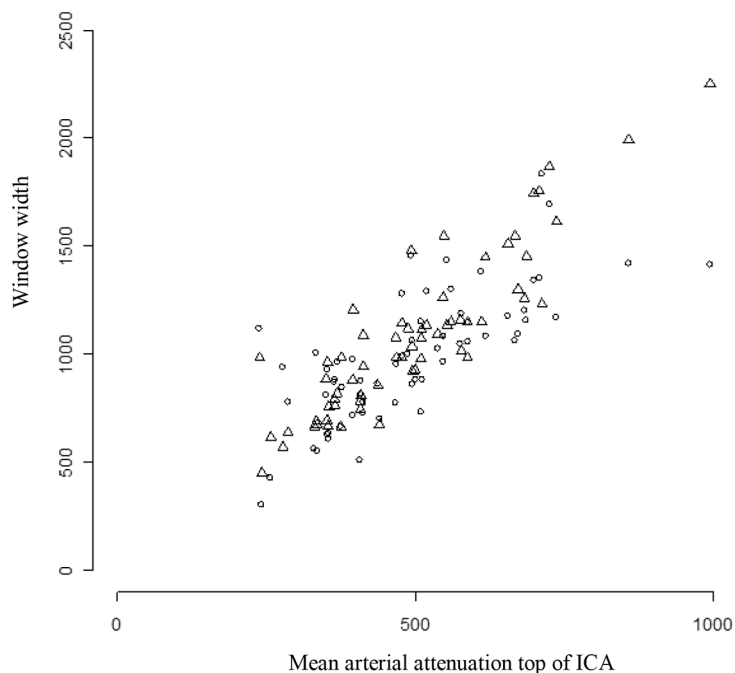


Fig.23 Scatter plot of chosen window width against mean arterial attenuation (HU) in the top of the ICA.  $\Delta$ =neuro-radiologist 1  $\circ$ =neuro-radiologist 2 (Paper II, Fig.3 reprinted with permission)

Image quality grading showed statistically improved grading for comparison of Group I to III (M1  $p=0.05$ ; M2  $p=0.02$ ; VR (M2)  $p=0.01$ ) whereas other group comparisons including general impression showed a trend towards higher mean grading values with increased iodine concentration and/or decreased tube voltage.

Based on the image quality grading and mean arterial attenuation in the ICA, a cut-off level for arterial attenuation for standard (grade 3) and excellent (grade 4) image quality was found at 340 HU in at least 90% of the examinations.

A calculation error was made in Paper II, however not affecting the results. In Table 7, the correct numbers and percentages are shown concerning the cut-off level for arterial attenuation.

Table 7. Image quality grading 1-4 concerning general impression (GI), volume rendering (VR), M1- and M2-segments of MCA, displaying the numbers and percentages at cut-off 340 HU compared to calculation error in Paper II.

	Grade 1-2	Grade 3-4		Grade 3-4	Grade 1-2
GI	90%(9/10)	10%(1/10)		90%(47/52)	10%(5/52)
VR	70%(7/10)	30%(3/10)	< 340 HU ≤	100%(52/52)	0%(0/52)
M1	87.5%(7/8)	12.5%(1/8)		93%(50/54)	7%(4/54)
M2	75%(6/8)	25%(2/8)		93%(50/54)	7%(4/54)



The measured phantom CTDI<sub>vol</sub> at tube voltage 90 kVp was 41.3 mGy (12.2% higher than displayed value) and at 120 kVp 38.2 mGy (16.8% higher).

The average eye lens dose was 41.1 mGy at 90 kVp and 35.3 mGy at 120 kVp.

## Paper III

Results regarding aneurysm detection with DSA in 326 patients are shown in Fig.24. In Table 8 location and size of aneurysm are shown.

266 out of 285 aneurysms were diagnosed on both DSA and CTA and of those 223 aneurysms were classified as ruptured.

Classification of aneurysms as true positive (seen on both CTA and DSA), true negative (no aneurysm either on CTA or DSA), false positive (suspected aneurysm on CTA but no aneurysm on DSA) and false negative (no aneurysm on CTA but true aneurysm on DSA) are given in Table 9.

Reviewing CTA examinations with false negative aneurysms showed that 10 aneurysms could be seen retrospectively, whereas 9 were not detectable (Table 10).

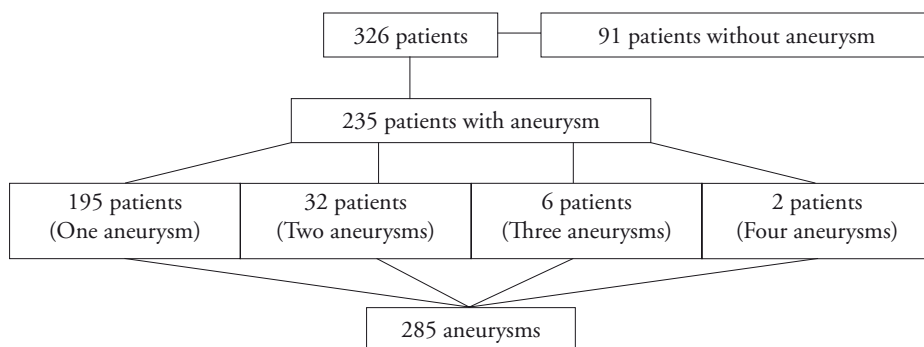


Fig.24 Patients and number of aneurysms identified by DSA.

**Table 8.** Location and size of aneurysms identified by DSA.

Location of aneurysm	Number of aneurysm	Size of aneurysm		
		≤ 2 mm	3-9 mm	≥ 10 mm
ACOM	103	6	88	9
ACA	3	-	3	-
PA	22	6	16	-
PCOM	41	-	38	3
ICA	22	1	19	2
MCA	41	10	28	3
BA	22	2	12	8
PICA	14	1	12	1
SCA	3	-	3	-
AICA	1	-	1	-
PCA	1	-	1	-
Pseudoaneurysms	12	2	6	4
<b>Total</b>	<b>285</b>	<b>28</b>	<b>227</b>	<b>30</b>

**Table 9.** Diagnostic agreement between CTA and DSA (gold standard) per patient, per aneurysm and per ruptured aneurysm.

	Diagnostic agreement between CTA and DSA (gold standard)			
	True positive	True negative	False positive	False negative
Per patient	209	87*	12 <sup>^</sup> *	19 <sup>^</sup>
Per aneurysm	266	88	12	19
Per ruptured aneurysm	223	88	3	12

\* One patient was suspected to have an ACOM aneurysm on CTA and had as well atherosclerosis; at DSA only atherosclerosis without aneurysm was seen

<sup>^</sup> In one patient a PCOM aneurysm was suspected on CTA, however, DSA showed an infundibulum instead and in the same patient a 2 mm aneurysm on PICA was missed on CTA

**Table 10.** Suspected cause of missed aneurysm (n=19), secondary detectability (n=10) and if the aneurysm was classified as ruptured or not.

Cause of missed aneurysm	Number of aneurysms	Secondary detectability	Aneurysms caused SAH (yes=1;no=0)
Second or third aneurysm, size 1-2 mm	6	3	0
Extradural aneurysm ICA	1	1	0
Blister- or pseudoaneurysms	3	0	1
Small size, 1-2 mm	3	2	1
Extensive SDH and SAH	1	1	1
Technically suboptimal CTA	3	3	1
Artefacts from adjacent coils or clips	2	0	1
<b>Total</b>	<b>19</b>	<b>10</b>	<b>12</b>

No significant difference for the two observer groups was seen regarding diagnostic accuracy of false negative and false positive aneurysms on CTA (non-interventional missing 8% of aneurysms and interventional missing 9%).

Sensitivity, specificity, accuracy, as well as positive and negative predictive values for detection of aneurysms with CTA is given in Table 11.

**Table 11.** Sensitivity, specificity, accuracy, and positive and negative predicted value of CTA calculated per patient, per aneurysm and per ruptured aneurysm levels.

	Sensitivity	Specificity	Accuracy	Positive predictive value	Negative predictive value
	% (95% confidence interval)				
Per patient	91.6 (87.3-94.9)	87.9 (79.8-93.6)	90.5 (86.8-93.5)	94.6 (90.7-97.2)	82.1 (73.4-88.8)
Per aneurysm	93.3 (89.7-95.9)	88.0 (79.9-93.6)	91.9 (88.8-94.5)	95.7 (92.9-97.7)	82.2 (73.7-89.0)
Per ruptured aneurysm	94.9 (91.3-97.3)	96.7 (90.7-99.3)	95.4 (92.5-97.4)	98.7 (96.2-99.7)	88.0 (80.0-93.6)

Mean (SD, range) arterial attenuation for all patients was 532 HU ( $\pm 110$ , 152-1062). Three patients were excluded from measurements due to unilateral ICA occlusion (n=1) or incomplete archiving of the CTA examinations in PACS (n=2).

One-way analysis of variance showed significant difference in arterial attenuation ( $p=0.02$ ) in patients with true positive aneurysms causing SAH and true negative aneurysms (mean  $535 \pm 110$  HU) compared with false negative aneurysms causing SAH (mean  $424 \pm 30$  HU).

Logistic regression analysis (Fig.25) showed a 50% probability to detect an aneurysm at a size of 2.2 mm at arterial attenuation  $< 340$  HU and at a size of 1.5 mm at  $\geq 340$  HU.

In Table12, the calculated probability to find an aneurysm on CTA is shown correlated to a logistic regression analysis.

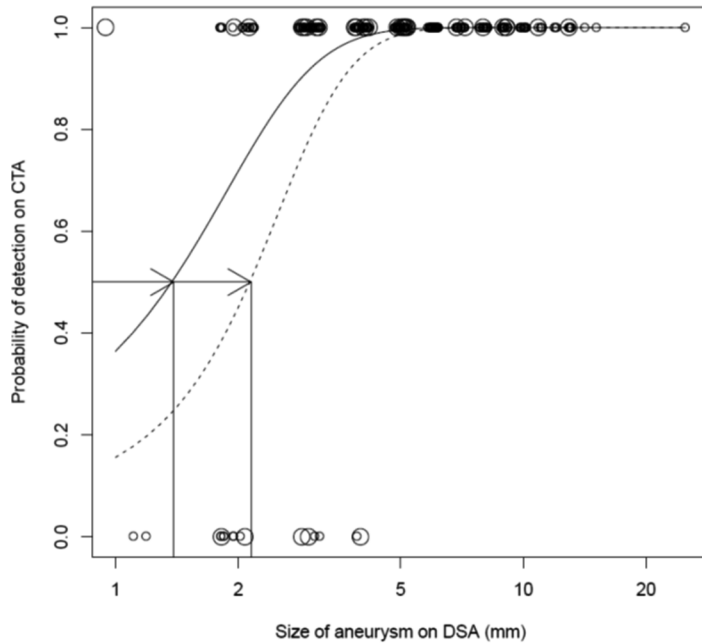


**Fig.25** Logistic regression analysis concerning aneurysm size and arterial attenuation (HU) on CTA correlated to < 340 HU (large rings) and  $\geq$  340 HU (small rings). The arrows at 0.5 show on the dotted line the probability to detect an aneurysm of a size of 2.2 mm on a CTA with arterial attenuation < 340 HU and on the solid line an aneurysm of a size of 1.5 mm at arterial attenuation  $\geq$  340 HU.

**Table 12.** Calculated probability (%) of detecting an aneurysm on CTA correlated to logistic regression of arterial attenuation (mean HU measured in ICA bilaterally).

	Aneurysm size – mm						
	1	2	3	4	5	6	7
<340 HU - %	15.8	45.0	78.4	94.1	98.6	99.7	99.9
$\geq$ 340 HU - %	36.4	71.8	91.9	98.0	99.6	99.9	100

The distribution of SAH patterns on non-enhanced CT according to the Fisher grading scale is illustrated in Table 13.

In 28 patients, a perimesencephalic pattern of SAH on non-enhanced CT was seen and in all of them a correct diagnoses was made with CTA.

**Table 13.** SAH in patients according to Fisher grading scale on non-enhanced CT

Fisher grade	1	2	3	4
Number of patients	20	23	170	113



# Discussion

## Main findings

The studies involved in this thesis showed that TOF-MRA at 3T has better agreement with DSA regarding follow-up of aneurysms treated with coils, than TOF-MRA at 1.5T and CE-MRA at 3T (Paper I). This has been confirmed by others<sup>60,61</sup>. A recent meta-analysis<sup>62</sup>, including Paper I, showed no significant difference between TOF-MRA and CE-MRA, indicating the former to be adequate in follow-up of coiled intracranial aneurysms.

Increased iodine concentration in contrast medium and decreased tube voltage improve image quality in CTA of intracranial arteries (Paper II). The positive effect of reduced tube voltage on image quality has further been described in a clinical study<sup>63</sup> as well as in phantom studies<sup>63,64</sup>. Furthermore, the effect of increased iodine concentration in contrast medium, especially in combination with decreased tube voltage, results in higher arterial attenuation<sup>63</sup> as described also in Paper II. Arterial attenuation in the ICA of 340 HU was found to represent a cut-off level, above which at least 90% of examinations were ranked as standard or excellent.

CTA can be performed with high sensitivity (95%) and specificity (97%) for detection of ruptured aneurysms in the acute setting of SAH (Paper III). This has also been described previously and complies with the latest meta-analysis presented<sup>65</sup>. The correlation of sensitivity on CTA to image quality, evaluated by arterial attenuation in the ICA, has not been done before in CTA of intracranial arteries.

## Inclusion criteria

In Paper I, the close proximity in time between TOF-MRAs at 1.5 and 3T, CE-MRA at 3T and DSA was valued as strength in the study design. However, it led to the discard of a further CE-MRA at 1.5T from the study protocol, as it would have implied further contrast doses in short proximity to the other given contrast doses. As CE-MRA at 1.5T had been previously described<sup>53,66</sup> this was not valued as a major drawback. TOF-MRA examinations performed after contrast applica-

tion<sup>67</sup> showed no significant advantage compared to non-enhanced TOF-MRA. Furthermore, disadvantages of enhancement in surrounding tissue and veins had been described for TOF-MRA<sup>68</sup>.

A fourth study group with the combination of low contrast medium concentration and low tube voltage in Paper II, would have been advantageous to further confirm the effect of contrast medium concentration seen in high tube voltage (120 kVp). It can be assumed that the effect is similar at lower kVp, possibly even more pronounced due to the k-edge effect. This has been shown for the thoracic region<sup>69</sup>. However, due to the incipient reinstallation of the scanner the study design was restricted to three study groups with different numbers of patients.

The number of patients included in Paper III could have been increased with widened inclusion criteria also accounting for patients examined with DSA at our institute, but with CTAs performed at other hospitals. However, the material included 326 patients and was comparable to a study<sup>59</sup> including 336 patients; otherwise the number of patients in published studies varies between 21–243 patients as presented in a recent meta-analysis<sup>28</sup>.

## DSA as gold standard

DSA as gold standard was performed with a state of the art method at the time, performed and evaluated by experienced or interventional neuroradiologists. 3D functionality was not performed in the clinical routine at the time for the follow-up of coiled aneurysms (Paper I). In Paper III, approximately 60% of the examinations were performed with both 2D and 3D DSA. The comparison between 2D and 3D DSA concerning small intracranial aneurysms, however, shows the superiority of 3D, especially with volume rendering<sup>70,71</sup> which could imply that small aneurysms were not diagnosed at the time.

It is a common method to measure the size of an aneurysm as the distance from the neck to the dome. In studies included in this thesis, measurements were performed on 2D images. For DSA measurements, it is important to have a measurement reference in the image, for example a catheter with known dimensions in a vessel. The angiographic catheter, however, was not always displayed in the angiograms in our studies, as the tip was often located outside the head and as proximal as possible in the arteries of the neck. In Paper I, therefore ICA and BA diameters were used as generally accepted measurement references (with assumed diameters of 4 mm and 3 mm, respectively).

## Contrast agents

Optimal contrast enhancement is a prerequisite for high diagnostic acceptability and requests optimal timing of contrast injections with adjusted contrast agent volume and as well as osmolality and viscosity. The used contrast-enhanced angiographic methods (CE-MRA, CTA and DSA) demand the contrast medium to be present in the arteries in an adequate dose during the whole scan duration, which makes it difficult to decrease given iodine- or gadolinium-based contrast agents. The goal in the clinical situation should be to minimize the scan time i.e. reduce radiation exposure in CTA, to minimize the risk of adverse events and to take in consideration the patient's cardiovascular and renal function.

In a recent study<sup>72</sup> performed on a 64-slice CT, low contrast doses (25 ml iomeprol 400 mgI/ml with 25 ml saline flush and injection speed 5 ml/s, compared to standard doses 50-80 ml, 20-40 ml saline flush and injection speed 5 ml/s) showed a sensitivity of 100% concerning the detection of aneurysms in non-traumatic SAH.

In CE-MRA, a standard dose is often given<sup>61</sup>, but if a dynamic sequence is used<sup>73</sup> the dose given is correlated to the body weight.

Beside contrast dose, timing of the contrast injection is crucial for optimal arterial enhancement. In Paper I, three examinations were not possible to evaluate because of vein filling due to bad contrast timing. This has also been described lately<sup>74</sup>, but in another study<sup>75</sup>, the only suboptimal images were two patients who had undergone stent placement or associated clipping. Furthermore, unnecessary use of contrast agents should be avoided not only due to the increased cost of an examination performed with contrast agents, but mainly due to the inherent risk of adverse events such as allergic reactions and renal insufficiency. When giving gadolinium-based contrast medium to patients with renal insufficiency, especially in combination with an inflammatory event, the risk of nephrogenic systemic fibrosis<sup>76</sup> needs to be taken into account.

## Image evaluation

In Paper I and II image evaluation was performed on dedicated workstations with the possibility to post process original data. Image evaluation for Paper III was hampered, as none-reconstructed thin slice data were not readily available for most patients, and therefore, the possibility to perform image post-processing was practically non-existing. This could affect our results concerning small aneurysms. However, out of 28 aneurysms being smaller than 3 mm in Paper III only 11 were not diagnosed on CTA, and therefore classified as false negative. This is in conformity with other studies presented, where the sensitivity of small aneurysms under 2 mm was



50%<sup>77</sup>, performed on 4-slice CT, and the sensitivity for aneurysms under 3 mm was 70.4%, performed on a 64-slice CT<sup>78</sup>.

CTAs in Paper III, had primarily been evaluated by experienced radiologists in neuroradiology – 3 interventional neuroradiologists, 11 neuroradiologists and 5 general radiologists in training for neuroradiology. Primary reading was performed during daytime, even if the examinations were performed during the night, unless an emergency response had been needed. No significant difference in diagnostic accuracy was seen between interventional and diagnostic neuroradiologists in evaluating images. A similar comparison has not been published, but a comparison between experienced neuroradiologists and non-neuroradiologists<sup>79</sup>, showed better performance, although not significant, for neuroradiologists. When investigating preliminary reports of on-call residents<sup>80</sup> regarding diagnostic performance for CTA in SAH aneurysm patients, 73% of aneurysms larger than 3 mm were diagnosed and 13% of all aneurysms were not detected. Sensitivity was poor for second aneurysms, as well as for aneurysms in localisations such as PCOM and ICA. However, a disadvantage for this study was the lacking possibility of 3D reconstructions and volume rendering at preliminary reading.

In patients with multiple aneurysms and SAH, it is usually possible to identify the ruptured aneurysm based on the distribution of the haemorrhage and the configuration of the aneurysm, e.g. its irregularity or bleeding nipple<sup>35</sup>. Ruptured aneurysms are usually larger compared to unruptured aneurysms (median 7 mm versus 3 mm)<sup>81</sup>. In Paper III, 40 patients had multiple aneurysms and the clinical decision on which aneurysm to treat could vary in difficulty. For example in one patient with two aneurysms, an irregular, 5 mm aneurysm located on PA was easily chosen for treatment over a round, 1 mm aneurysm on the callosomarginal artery. In another patient, the ruptured aneurysm could not be safely identified and both an irregular 8 mm aneurysm, close to the origin of the choroidal artery from the ICA and a 9 mm aneurysm at the top of the ICA were treated in the acute phase to prevent rebleeding.

Concerning endovascular devices (other than coils) as for example intracranial stents, the follow-up examinations could be CE-MRA<sup>82</sup> or TOF-MRA<sup>83</sup> as well as DSA. In the combination of stent and coils, the data reconstruction from gated CTA has been showed to be able to minimize the streak artefacts from coils<sup>84</sup>, giving a possibility to examine these patients with a non-invasive method. Also for the follow-up examinations of flow-diverters, usually MRI is used for evaluation of the aneurysm and DSA for evaluation of the parent artery<sup>85</sup>. With the new intrasaccular flow disrupter, still DSA is the modality for the follow-up.

## Grading scales

In CTA, being a modality using ionizing radiation, it is advantageous to use a four-graded scale in order to distinguish between none-diagnostic, poor, standard and excellent examinations, as was used in Paper I. This allows not only the identification of none-diagnostic examinations that should be repeated, but also to identify a general overexposure to ionizing radiation, yielding exams that are better than anticipated and necessary.

As CTA examinations performed for the papers included in this thesis were performed between 2005-2011, reported  $CTDI_{vol}$  are higher (Paper II 32.6 and 36.8 mGy; Paper III 23.5-37.8 mGy) than expected for modern scanners yielding  $CTDI_{vol}$  of approximately 23 mGy and even as low as 13 mGy<sup>63</sup>. Decreasing exposure levels are mainly explained by advances in software developments such as new and more efficient reconstruction algorithms and are heavily demanded considering a widening of examination indications and rising number of examinations in general.

When comparing new or improved techniques to gold standard methods it is often desirable to be able to grade even small differences in technical advances. In Paper I, a modified Raymond classification with five instead of four grades was used, mainly because of the focus on comparing different MR techniques. When Paper I was included in a meta-analysis<sup>62</sup> a translation to the original Raymond classification with the grading obliteration, “dog ear”, residual neck and residual aneurysm was made.

Concerning regrowth (enlargement of the aneurysm) in comparison to recanalization (coil compaction) of a coiled aneurysm, we defined in Paper I, regrowth as a 20% enlargement of the aneurysm compared to the initial size, as no accepted definition existed at the time of publication. In a newly published article<sup>86</sup>, an arbitrary cut-off of 30% was used for regrowth, which could decrease the sensitivity for small aneurysm recurrences. Special software was used in this study to measure size by means of number of pixels covering the area of the aneurysm. However, if either the cut-off of 20% or 30% was used for the definition of regrowth, it did not change our results.

## Image quality grading

Image evaluation biases are important to avoid. Recognition bias can be decreased if repeated image evaluations are done with sufficient time in between (Paper I) or grading of image quality is performed randomly and blinded for important information (Paper II).

Observer bias is pronounced if no thorough definitions of evaluation criteria and training of the grading scale prior to image evaluation are provided, which were accomplished in Paper I and II before image quality grading. Confirmation bias has to be considered if the observers themselves are responsible for the study design, which were partly the case in all three studies included in this thesis.

Both individual and consensus grading have inherent disadvantages. Inter-observer variation showed poor agreement between two observers for example concerning residue in a silicon model evaluated with TOF-MRA<sup>87</sup>. If consensus grading is performed due to poor agreement between independent observers, as in Paper I, there is a risk of one observer's opinion becoming more dominant, resulting in an increased observer bias. In Paper I, one of the observers was interventional and two were diagnostic neuroradiologists, which meant that the interventional neuro-radiologist was more experienced to assess recanalization of coiled aneurysms.

Due to these known image evaluation biases, it is advantageous to imply objective image quality parameters, as for example arterial attenuation for CTA of intracranial arteries. This has been done earlier for pulmonary CTA, but to my knowledge not for intracranial CTA. When studying bodyweight and scan duration<sup>88</sup>, a minimum level of pulmonary artery enhancement required for assessing the diagnosis of pulmonary emboli was 250 HU. The threshold of 250 HU was used<sup>89</sup> to evaluate, if a reduced contrast dose from 125 ml to 75 ml 370 mgI/ml and low tube voltage could give equivalent opacification in all vessels in pulmonary CTA. In both groups all vessels were observed at an attenuation level above 250 HU.

In Paper II, it was attempted to find a cut-off for arterial attenuation at which at least 90% of examinations were graded as standard or excellent. The cut-off level found was 340 HU in ICA and when the cut-off level was used in Paper III, the calculated probability to detect a 2 mm aneurysm on an examination with arterial attenuation <340 HU was 45% compared to 72% for an examination with arterial attenuation  $\geq 340$  HU.

Arterial attenuation was >340 HU in examinations with 13 out of the 19 false negative aneurysms and with 9 out of the 12 false positive aneurysms in Paper III. This indicates also other factors such as localisation and size of the aneurysm, early filling of adjacent veins and different assessment biases<sup>90,91</sup> need to be considered.

Assessment of arterial attenuation in ICA bilaterally, as in Paper II and III, was recently performed in a similar setting<sup>63</sup> although iodine concentrations of 300 and 370 mgI/ml were used. Mean arterial attenuation was 379 HU for the 80 kVp protocol and 282 HU for the 120 kVp protocol. These arterial attenuation values are significantly lower than ours (90 kVp protocol – 579 HU and 120 kVp protocol 360-424 HU) and a probable explanation is the use of a 64-slice CT and dose modulation. The displayed CTDI<sub>vol</sub> was 17.2 mGy for 120 kVp and 13.2 mGy for 80 kVp protocol, which is considerable lower than displayed CTDI<sub>vol</sub> in our studies (23.5-36.8 mGy). This illustrates well how fast developments in CT technique can change dose indexes.

In Paper I, susceptibility artefacts from the coil mesh on MRA are larger on TOF-MRA at 1.5T than at 3T, probably due to higher bandwidth and shorter TE used at 3T, which was also shown in a recent published study<sup>92</sup>. To minimize coil artefacts is important, as coil visibility is important when evaluating regrowth or recanalization as well as the relationship between the coil mesh and residual flow<sup>61</sup>.

## Clinical implications

Using the defined pattern of perimesencephalic haemorrhage<sup>93</sup> in patients with SAH, a subgroup of 28 patients were identified in Paper III showing this type of SAH. Our results are in line with other studies<sup>94-97</sup> and considering the combined results, it can be concluded that CTA is an accurate diagnostic method to rule out aneurysms in patients with a perimesencephalic pattern of haemorrhage on non-enhanced CT.

Another important issue are patients with clinical symptoms of SAH but showing Fisher grade 1 (no haemorrhage) on non-enhanced CT. If lumbar puncture in these cases indicates suspicion of haemorrhage, is CTA sufficient to rule out a ruptured aneurysm as origin for the SAH? In Paper III, 20 patients had SAH Fisher grade 1 and 17 of them had no aneurysm. In two patients, an aneurysm each was found on CTA and one patient had a false positive ACOM aneurysm being diagnosed as a fenestration on DSA. Our results were confirmed recently<sup>95,98</sup> and thus in this situation, there is no need to perform DSA but a thorough discussion concerning the patient's symptoms is important before the final decision.

## Future aspects

With the continuing advances in CT as well as MR technology, there will be new updates and versions to evaluate in correlation to established technics today and even probably new uses.

There will also be further developments of endovascular devices and it is important to continue to evaluate non-invasive follow-up examinations.



# Conclusions

## Paper I

- MRA, being a non-invasive method without using ionizing radiation, can be used for follow-up of intracranial aneurysms treated endovascularly with coils. TOF-MRA at 3T showed better agreement with the gold standard DSA than TOF-MRA at 1.5T and CE-MRA at 3T.

## Paper II

- Increased iodine concentration (400 mgI/ml) and decreased tube voltage (90 kVp) improved image quality in CTA of intracranial arteries and arterial attenuation at 340 HU in the ICA was found to represent a cut-off level for examinations of good quality.

## Paper III

- CTA can be performed with high sensitivity (95%) and specificity (97%) for the detection of ruptured aneurysms in the acute setting of SAH and arterial attenuation is correlated to the sensitivity.



# Recommendations and impact on clinical routine

- We recommend and perform TOF-MRA for follow-up of endovascularly treated aneurysms with coils and if possible on a 3T MR scanner. In ambiguous cases, a supplementary DSA should be performed for evaluation of potential retreatment.
- For CTA of intracranial arteries, we recommend and use in clinical routine highly concentrated contrast medium in combination with low tube voltage to optimize image quality.
- We recommend that if the patient's clinical status is consistent with a CTA of good quality, it will be the only examination performed for the decision of treatment. However, if CTA has poor image quality and no aneurysms are found in a patient with SAH, the patient should undergo a new CTA or DSA.
- CTA of intracranial arteries is an accurate diagnostic tool to rule out aneurysms in patients with perimesencephalic pattern of SAH on non-enhanced CT.





# Acknowledgements

I wish to express my sincere gratitude and many thanks to all who have supported and helped me in my studies and with the completion of this thesis. In particular I would like to thank:

Associate Professor Isabella Björkman-Burtscher, my senior supervisor, for believing in me and for your excellent scientific training and guidance.

Professor Elna-Marie Larsson and Associate Professor Kasim Abul-Kasim, my two co supervisors, for their support and well thought-out advices concerning my research.

Dr Peter Hochbergs, Chief of Department of Medical Imaging and Physiology and Professor Pia Maly-Sundgren, whom have been giving me support to my academic efforts with both time and encouragement.

Professors Stig Holtås and Peter Höglund, Associate Professors Ola Nilsson and Roger Siemund, Drs Mats Cronqvist and Per Undrén, my other co-authors, for your invaluable advices.

All present and earlier colleagues, who over the years have been working at the Section of Neuroradiology and been giving me support and the possibility to do research. None mentioned, none forgotten!

All radiographers, medical physicists, secretaries and administrators, for giving me a tremendous support and assistance in my daily neurointerventional work as well as research, with special thanks to:

Eva Hallberg, Inga-Lill Enocksson, Lena Kulstad, Boel Hansson, Titti Owman, Johan Olsrud and Nuray Güner for help with Paper I.

In Paper II, especially Mette Forseth and Lars Weber have been a great help.

For the administration needed in my research, I would like to thank Susanne Larsson Lleshdedaj, Monica Pedersen, Halina Vahabi and Annika Törling-Ring.

Then, I would like to thank Amir Vahabi, Göran Winholt and Gunnar Gunnarsson, for all their help with images and photos.

Furthermore, assisting me in my daily work at Section of Neuroradiology, I would like to thank Gunilla Angelin, Eva Borglin, Åsa Hansson, Karolina Larsson, Ann Olsson, Constance Persson, Oskar Rundgren, Helena Szaboova, Siv Tjärnberg, Alexandra Trudel, Pia Weijdegård and once again Göran Winholt, Amir Vahabi and Mette Forseth. My apologies if I have forgotten anyone!

Also, I would like to thank all my friends who still puts up with me, especially during the last few years. Special thanks to my friends Kerstin and Carl Hampus Lyttkens for your patience and advices!

Finally, I would like to thank my family and especially my beloved husband Jens, for you being there and encouraging me – I love you and can't live without you!

# References

1. Rinkel GJ, Djibuti M, Algra A, van Gijn J. Prevalence and risk of rupture of intracranial aneurysms: a systematic review. *Stroke; a journal of cerebral circulation*. Jan 1998;29(1):251-256.
2. de Rooij NK, Linn FH, van der Plas JA, Algra A, Rinkel GJ. Incidence of subarachnoid haemorrhage: a systematic review with emphasis on region, age, gender and time trends. *Journal of neurology, neurosurgery, and psychiatry*. Dec 2007;78(12):1365-1372.
3. Koffijberg H, Buskens E, Granath F, et al. Subarachnoid haemorrhage in Sweden 1987-2002: regional incidence and case fatality rates. *Journal of neurology, neurosurgery, and psychiatry*. Mar 2008;79(3):294-299.
4. Linn FH, Rinkel GJ, Algra A, van Gijn J. Incidence of subarachnoid hemorrhage: role of region, year, and rate of computed tomography: a meta-analysis. *Stroke; a journal of cerebral circulation*. Apr 1996;27(4):625-629.
5. Hop JW, Rinkel GJ, Algra A, van Gijn J. Case-fatality rates and functional outcome after subarachnoid hemorrhage: a systematic review. *Stroke; a journal of cerebral circulation*. Mar 1997;28(3):660-664.
6. Nieuwkamp DJ, Setz LE, Algra A, Linn FH, de Rooij NK, Rinkel GJ. Changes in case fatality of aneurysmal subarachnoid haemorrhage over time, according to age, sex, and region: a meta-analysis. *Lancet neurology*. Jul 2009;8(7):635-642.
7. Beseoglu K, Holtkamp K, Steiger HJ, Hanggi D. Fatal aneurysmal subarachnoid haemorrhage: causes of 30-day in-hospital case fatalities in a large single-centre historical patient cohort. *Clinical neurology and neurosurgery*. Jan 2013;115(1):77-81.
8. Molyneux A, Kerr R, Stratton I, et al. International Subarachnoid Aneurysm Trial (ISAT) of neurosurgical clipping versus endovascular coiling in 2143 patients with ruptured intracranial aneurysms: a randomised trial. *Lancet*. Oct 26 2002;360(9342):1267-1274.
9. Wiebers DO, Whisnant JP, Huston J, 3rd, et al. Unruptured intracranial aneurysms: natural history, clinical outcome, and risks of surgical and endovascular treatment. *Lancet*. Jul 12 2003;362(9378):103-110.
10. Cloft HJ, Joseph GJ, Dion JE. Risk of cerebral angiography in patients with subarachnoid hemorrhage, cerebral aneurysm, and arteriovenous malformation: a meta-analysis. *Stroke; a journal of cerebral circulation*. Feb 1999;30(2):317-320.

11. Willinsky RA, Taylor SM, TerBrugge K, Farb RI, Tomlinson G, Montanera W. Neurologic complications of cerebral angiography: prospective analysis of 2,899 procedures and review of the literature. *Radiology*. May 2003;227(2):522-528.
12. Dawkins AA, Evans AL, Wattam J, et al. Complications of cerebral angiography: a prospective analysis of 2,924 consecutive procedures. *Neuroradiology*. Sep 2007;49(9):753-759.
13. Thiex R, Norbash AM, Frerichs KU. The safety of dedicated-team catheter-based diagnostic cerebral angiography in the era of advanced noninvasive imaging. *AJNR. American journal of neuroradiology*. Feb 2010;31(2):230-234.
14. Zhang H, Hou C, Zhou Z, Zhang H, Zhou G, Zhang G. Evaluating of Small Intracranial Aneurysms by 64-Detector CT Angiography: A Comparison with 3-Dimensional Rotation DSA or Surgical Findings. *Journal of Neuroimaging*. 2014;24(2):137-143.
15. Wang H, Li W, He H, Luo L, Chen C, Guo Y. 320-Detector row CT angiography for detection and evaluation of intracranial aneurysms: Comparison with conventional digital subtraction angiography. *Clinical radiology*. 1// 2013;68(1):e15-e20.
16. Li Q, Lv F, Wei Y, Luo T, Xie P. Automated subtraction CT angiography for visualization of the whole brain vasculature: a feasibility study. *Academic radiology*. Aug 2013;20(8):1009-1014.
17. Luo Z, Wang D, Sun X, et al. Comparison of the accuracy of subtraction CT angiography performed on 320-detector row volume CT with conventional CT angiography for diagnosis of intracranial aneurysms. *European journal of radiology*. Jan 2012;81(1):118-122.
18. Sailer AM, Wagemans BA, Nelemans PJ, de Graaf R, van Zwam WH. Diagnosing intracranial aneurysms with MR angiography: systematic review and meta-analysis. *Stroke; a journal of cerebral circulation*. Jan 2014;45(1):119-126.
19. Gibbs GF, Huston J, 3rd, Bernstein MA, Riederer SJ, Brown RD, Jr. 3.0-Tesla MR angiography of intracranial aneurysms: comparison of time-of-flight and contrast-enhanced techniques. *Journal of magnetic resonance imaging: JMRI*. Feb 2005;21(2):97-102.
20. Numminen J, Tarkiainen A, Niemela M, Porras M, Hernesniemi J, Kangasniemi M. Detection of unruptured cerebral artery aneurysms by MRA at 3.0 tesla: comparison with multislice helical computed tomographic angiography. *Acta radiologica (Stockholm, Sweden: 1987)*. Jul 1 2011;52(6):670-674.
21. Cirillo M, Scomazzoni F, Cirillo L, et al. Comparison of 3D TOF-MRA and 3D CE-MRA at 3T for imaging of intracranial aneurysms. *European journal of radiology*. Dec 2013;82(12):e853-859.
22. Moniz E. Cerebral angiography its application in clinical practice and physiology. *Lancet*. nov 18 1933:1144-1147.
23. Seldinger SI. Catheter replacement of the needle in percutaneous arteriography; a new technique. *Acta radiologica (Stockholm, Sweden: 1987)*. May 1953;39(5):368-376.

24. Serbinenko FA. Balloon catheterization and occlusion of major cerebral vessels. *Journal of neurosurgery*. Aug 1974;41(2):125-145.
25. Guglielmi G, Vinuela F, Sepetka I, Macellari V. Electrothrombosis of saccular aneurysms via endovascular approach. Part 1: Electrochemical basis, technique, and experimental results. *Journal of neurosurgery*. Jul 1991;75(1):1-7.
26. Anzalone N, Scomazzoni F, Cirillo M, et al. Follow-up of coiled cerebral aneurysms at 3T: comparison of 3D time-of-flight MR angiography and contrast-enhanced MR angiography. *AJNR. American journal of neuroradiology*. Sep 2008;29(8):1530-1536.
27. Agid R, Lee SK, Willinsky RA, Farb RI, terBrugge KG. Acute subarachnoid hemorrhage: using 64-slice multidetector CT angiography to “triage” patients’ treatment. *Neuroradiology*. Nov 2006;48(11):787-794.
28. Westerlaan HE, van Dijk JMC, Jansen-van der Weide MC, et al. Intracranial Aneurysms in Patients with Subarachnoid Hemorrhage: CT Angiography as a Primary Examination Tool for Diagnosis – Systematic Review and Meta-Analysis. *Radiology*. 2011;258(1):134-145.
29. Iqbal S. A comprehensive study of the anatomical variations of the circle of willis in adult human brains. *Journal of clinical and diagnostic research: JCDR*. Nov 2013;7(11):2423-2427.
30. Kapoor K, Singh B, Dewan LI. Variations in the configuration of the circle of Willis. *Anatomical science international*. Jun 2008;83(2):96-106.
31. Fifi JT, Meyers PM, Lavine SD, et al. Complications of modern diagnostic cerebral angiography in an academic medical center. *Journal of vascular and interventional radiology: JVIR*. Apr 2009;20(4):442-447.
32. Brisman JL, Song JK, Newell DW. Cerebral aneurysms. *The New England journal of medicine*. Aug 31 2006;355(9):928-939.
33. Wiebers DO, Piepgras DG, Meyer FB, et al. Pathogenesis, natural history, and treatment of unruptured intracranial aneurysms. *Mayo Clinic proceedings*. Dec 2004;79(12):1572-1583.
34. Wermer MJ, van der Schaaf IC, Algra A, Rinkel GJ. Risk of rupture of unruptured intracranial aneurysms in relation to patient and aneurysm characteristics: an updated meta-analysis. *Stroke; a journal of cerebral circulation*. Apr 2007;38(4):1404-1410.
35. Nehls DG, Flom RA, Carter LP, Spetzler RF. Multiple intracranial aneurysms: determining the site of rupture. *Journal of neurosurgery*. Sep 1985;63(3):342-348.
36. Rinne J, Hernesniemi J, Puranen M, Saari T. Multiple intracranial aneurysms in a defined population: prospective angiographic and clinical study. *Neurosurgery*. Nov 1994;35(5):803-808.
37. Juvola S. Risk factors for multiple intracranial aneurysms. *Stroke; a journal of cerebral circulation*. Feb 2000;31(2):392-397.
38. Kayembe KN, Sasahara M, Hazama F. Cerebral aneurysms and variations in the circle of Willis. *Stroke; a journal of cerebral circulation*. Sep-Oct 1984;15(5):846-850.

39. Gross BA, Du R. Natural history of cerebral arteriovenous malformations: a meta-analysis. *Journal of neurosurgery*. Feb 2013;118(2):437-443.
40. Birnbaum J, Hellmann DB. Primary angitis of the central nervous system. *Archives of neurology*. Jun 2009;66(6):704-709.
41. Touze E, Oppenheim C, Trystram D, et al. Fibromuscular dysplasia of cervical and intracranial arteries. *International journal of stroke: official journal of the International Stroke Society*. Aug 2010;5(4):296-305.
42. Burke GM, Burke AM, Sherma AK, Hurley MC, Batjer HH, Bendok BR. Moyamoya disease: a summary. *Neurosurgical focus*. Apr 2009;26(4):E11.
43. Ducros A, Boukobza M, Porcher R, Sarov M, Valade D, Bousser MG. The clinical and radiological spectrum of reversible cerebral vasoconstriction syndrome. A prospective series of 67 patients. *Brain: a journal of neurology*. Dec 2007;130(Pt 12):3091-3101.
44. Fisher CM, Kistler JP, Davis JM. Relation of cerebral vasospasm to subarachnoid hemorrhage visualized by computerized tomographic scanning. *Neurosurgery*. Jan 1980;6(1):1-9.
45. Karttunen AI, Jartti PH, Ukkola VA, Sajanti J, Haaepa M. Value of the quantity and distribution of subarachnoid haemorrhage on CT in the localization of a ruptured cerebral aneurysm. *Acta neurochirurgica*. Aug 2003;145(8):655-661; discussion 661.
46. Wilson FM, Jaspan T, Holland IM. Multiple cerebral aneurysms--a reappraisal. *Neuroradiology*. 1989;31(3):232-236.
47. Kaminogo M, Yonekura M, Shibata S. Incidence and outcome of multiple intracranial aneurysms in a defined population. *Stroke; a journal of cerebral circulation*. Jan 2003;34(1):16-21.
48. Cognard C, Weill A, Spelle L, et al. Long-term angiographic follow-up of 169 intracranial berry aneurysms occluded with detachable coils. *Radiology*. Aug 1999;212(2):348-356.
49. Raymond J, Guilbert F, Weill A, et al. Long-term angiographic recurrences after selective endovascular treatment of aneurysms with detachable coils. *Stroke; a journal of cerebral circulation*. Jun 2003;34(6):1398-1403.
50. Weber W, Yousry TA, Felber SR, et al. Noninvasive follow-up of GDC-treated saccular aneurysms by MR angiography. *European radiology*. 2001;11(9):1792-1797.
51. Okahara M, Kiyosue H, Yamashita M, et al. Diagnostic accuracy of magnetic resonance angiography for cerebral aneurysms in correlation with 3D-digital subtraction angiographic images: a study of 133 aneurysms. *Stroke; a journal of cerebral circulation*. Jul 2002;33(7):1803-1808.
52. Nome T, Bakke SJ, Nakstad PH. MR angiography in the follow-up of coiled cerebral aneurysms after treatment with Guglielmi detachable coils. *Acta radiologica (Stockholm, Sweden: 1987)*. Jan 2002;43(1):10-14.
53. Gauvrit JY, Leclerc X, Caron S, Taschner CA, Lejeune JP, Pruvo JP. Intracranial aneurysms treated with Guglielmi detachable coils: imaging follow-up with

- contrast-enhanced MR angiography. *Stroke; a journal of cerebral circulation*. Apr 2006;37(4):1033-1037.
54. Cottier JP, Bleuzen-Couthon A, Gallas S, et al. Follow-up of intracranial aneurysms treated with detachable coils: comparison of plain radiographs, 3D time-of-flight MRA and digital subtraction angiography. *Neuroradiology*. Nov 2003;45(11):818-824.
  55. Farb RI, Nag S, Scott JN, et al. Surveillance of intracranial aneurysms treated with detachable coils: a comparison of MRA techniques. *Neuroradiology*. Jul 2005;47(7):507-515.
  56. Gibbs GF, Huston J, 3rd, Bernstein MA, Riederer SJ, Brown RD, Jr. Improved image quality of intracranial aneurysms: 3.0-T versus 1.5-T time-of-flight MR angiography. *AJNR. American journal of neuroradiology*. Jan 2004;25(1):84-87.
  57. Ertl-Wagner BB, Hoffmann RT, Bruning R, et al. Multi-detector row CT angiography of the brain at various kilovoltage settings. *Radiology*. May 2004;231(2):528-535.
  58. Pedersen HK, Bakke SJ, Hald JK, et al. CTA in patients with acute subarachnoid haemorrhage. A comparative study with selective, digital angiography and blinded, independent review. *Acta radiologica (Stockholm, Sweden: 1987)*. Jan 2001;42(1):43-49.
  59. Colen TW, Wang LC, Ghodke BV, Cohen WA, Hollingworth W, Anzai Y. Effectiveness of MDCT Angiography for the Detection of Intracranial Aneurysms in Patients with Nontraumatic Subarachnoid Hemorrhage. *American Journal of Roentgenology*. 2007/10/01 2007;189(4):898-903.
  60. Ferre JC, Carsin-Nicol B, Morandi X, et al. Time-of-flight MR angiography at 3T versus digital subtraction angiography in the imaging follow-up of 51 intracranial aneurysms treated with coils. *European journal of radiology*. Dec 2009;72(3):365-369.
  61. Pierot L, Portefaix C, Boulin A, Gauvrit JY. Follow-up of coiled intracranial aneurysms: comparison of 3D time-of-flight and contrast-enhanced magnetic resonance angiography at 3T in a large, prospective series. *European radiology*. Oct 2012;22(10):2255-2263.
  62. van Amerongen MJ, Boogaarts HD, de Vries J, et al. MRA Versus DSA for Follow-Up of Coiled Intracranial Aneurysms: A Meta-Analysis. *AJNR. American journal of neuroradiology*. Sep 5 2013.
  63. Cho ES, Chung TS, Oh DK, et al. Cerebral computed tomography angiography using a low tube voltage (80 kVp) and a moderate concentration of iodine contrast material: a quantitative and qualitative comparison with conventional computed tomography angiography. *Investigative radiology*. Feb 2012;47(2):142-147.
  64. Papadakis AE, Perisinakis K, Raissaki M, Damilakis J. Effect of x-ray tube parameters and iodine concentration on image quality and radiation dose in cerebral pediatric and adult CT angiography: a phantom study. *Investigative radiology*. Apr 2013;48(4):192-199.
  65. Westerlaan HE, van Dijk JM, Jansen-van der Weide MC, et al. Intracranial aneurysms in patients with subarachnoid hemorrhage: CT angiography as a primary



- examination tool for diagnosis--systematic review and meta-analysis. *Radiology*. Jan 2011;258(1):134-145.
66. Leclerc X, Navez JF, Gauvrit JY, Lejeune JP, Pruvo JP. Aneurysms of the anterior communicating artery treated with Guglielmi detachable coils: follow-up with contrast-enhanced MR angiography. *AJNR. American journal of neuroradiology*. Aug 2002;23(7):1121-1127.
  67. Wikstrom J, Ronne-Engstrom E, Gal G, Enblad P, Tovi M. Three-dimensional time-of-flight (3D TOF) magnetic resonance angiography (MRA) and contrast-enhanced MRA of intracranial aneurysms treated with platinum coils. *Acta radiologica (Stockholm, Sweden: 1987)*. Mar 2008;49(2):190-196.
  68. Ozsarlak O, Van Goethem JW, Maes M, Parizel PM. MR angiography of the intracranial vessels: technical aspects and clinical applications. *Neuroradiology*. Dec 2004;46(12):955-972.
  69. Szucs-Farkas Z, Verdun FR, von Allmen G, Mini RL, Vock P. Effect of X-ray tube parameters, iodine concentration, and patient size on image quality in pulmonary computed tomography angiography: a chest-phantom-study. *Investigative radiology*. Jun 2008;43(6):374-381.
  70. van Rooij WJ, Sprengers ME, de Gast AN, Peluso JP, Sluzewski M. 3D rotational angiography: the new gold standard in the detection of additional intracranial aneurysms. *AJNR. American journal of neuroradiology*. May 2008;29(5):976-979.
  71. Shi WY, Li YD, Li MH, et al. 3D rotational angiography with volume rendering: the utility in the detection of intracranial aneurysms. *Neurology India*. Nov-Dec 2010;58(6):908-913.
  72. Millon D, Derelle AL, Omoumi P, et al. Nontraumatic subarachnoid hemorrhage management: evaluation with reduced iodine volume at CT angiography. *Radiology*. Jul 2012;264(1):203-209.
  73. Serafin Z, Strzesniewski P, Lasek W, Beuth W. Time-resolved imaging of contrast kinetics does not improve performance of follow-up MRA of embolized intracranial aneurysms. *Medical science monitor: international medical journal of experimental and clinical research*. Jul 2012;18(7):Mt60-65.
  74. Sprengers ME, Schaafsma JD, van Rooij WJ, et al. Evaluation of the occlusion status of coiled intracranial aneurysms with MR angiography at 3T: is contrast enhancement necessary? *AJNR. American journal of neuroradiology*. Oct 2009;30(9):1665-1671.
  75. Shankar JJ, Lum C, Parikh N, dos Santos M. Long-term prospective follow-up of intracranial aneurysms treated with endovascular coiling using contrast-enhanced MR angiography. *AJNR. American journal of neuroradiology*. Aug 2010;31(7):1211-1215.
  76. Sadowski EA, Bennett LK, Chan MR, et al. Nephrogenic systemic fibrosis: risk factors and incidence estimation. *Radiology*. Apr 2007;243(1):148-157.
  77. Wintermark M, Uske A, Chalaron M, et al. Multislice computerized tomography angiography in the evaluation of intracranial aneurysms: a comparison with

- intraarterial digital subtraction angiography. *Journal of neurosurgery*. Apr 2003;98(4):828-836.
78. Lubicz B, Levivier M, Francois O, et al. Sixty-four-row multisection CT angiography for detection and evaluation of ruptured intracranial aneurysms: interobserver and intertechnique reproducibility. *AJNR. American journal of neuroradiology*. Nov-Dec 2007;28(10):1949-1955.
  79. White PM, Wardlaw JM, Lindsay KW, Sloss S, Patel DK, Teasdale EM. The non-invasive detection of intracranial aneurysms: are neuroradiologists any better than other observers? *European radiology*. Feb 2003;13(2):389-396.
  80. Hochberg AR, Rojas R, Thomas AJ, Reddy AS, Bhadelia RA. Accuracy of on-call resident interpretation of CT angiography for intracranial aneurysm in subarachnoid hemorrhage. *AJR. American journal of roentgenology*. Dec 2011;197(6):1436-1441.
  81. Huttunen T, von und zu Fraunberg M, Frosen J, et al. Saccular intracranial aneurysm disease: distribution of site, size, and age suggests different etiologies for aneurysm formation and rupture in 316 familial and 1454 sporadic eastern Finnish patients. *Neurosurgery*. Apr 2010;66(4):631-638; discussion 638.
  82. Agid R, Schaaf M, Farb R. CE-MRA for follow-up of aneurysms post stent-assisted coiling. *Interventional neuroradiology: journal of peritherapeutic neuroradiology, surgical procedures and related neurosciences*. Sep 2012;18(3):275-283.
  83. Cho YD, Kim KM, Lee WJ, et al. Time-of-flight magnetic resonance angiography for follow-up of coil embolization with enterprise stent for intracranial aneurysm: usefulness of source images. *Korean journal of radiology: official journal of the Korean Radiological Society*. Jan-Feb 2014;15(1):161-168.
  84. Kovacs A, Mohlenbruch M, Hadizadeh DR, et al. Noninvasive imaging after stent-assisted coiling of intracranial aneurysms: comparison of 3-T magnetic resonance imaging and 64-row multidetector computed tomography – a pilot study. *Journal of computer assisted tomography*. Sep-Oct 2011;35(5):573-582.
  85. Saatci I, Yavuz K, Ozer C, Geyik S, Cekirge HS. Treatment of intracranial aneurysms using the pipeline flow-diverter embolization device: a single-center experience with long-term follow-up results. *AJNR. American journal of neuroradiology*. Sep 2012;33(8):1436-1446.
  86. Abdihalim M, Watanabe M, Chaudhry SA, Jagadeesan B, Suri MF, Qureshi AI. Are coil compaction and aneurysmal growth two distinct etiologies leading to recurrence following endovascular treatment of intracranial aneurysm? *Journal of neuroimaging: official journal of the American Society of Neuroimaging*. Mar 2014;24(2):171-175.
  87. Costalat V, Lebars E, Sarry L, et al. In Vitro Evaluation of 2D-Digital Subtraction Angiography versus 3D-Time-of-Flight in Assessment of Intracranial Cerebral Aneurysm Filling after Endovascular Therapy. *American Journal of Neuroradiology*. January 1, 2006 2006;27(1):177-184.
  88. Bae KT, Tao C, Gurel S, et al. Effect of patient weight and scanning duration on contrast enhancement during pulmonary multidetector CT angiography. *Radiology*. Feb 2007;242(2):582-589.

89. Hunsaker AR, Oliva IB, Cai T, et al. Contrast opacification using a reduced volume of iodinated contrast material and low peak kilovoltage in pulmonary CT angiography: Objective and subjective evaluation. *AJR. American journal of roentgenology*. Aug 2010;195(2):W118-124.
90. Donmez H, Serifov E, Kahriman G, Mavili E, Durak AC, Menku A. Comparison of 16-row multislice CT angiography with conventional angiography for detection and evaluation of intracranial aneurysms. *European journal of radiology*. Nov 2011;80(2):455-461.
91. Love A, Siemund R, Hoglund P, Ramgren B, Undren P, Bjorkman-Burtscher IM. Hybrid iterative reconstruction algorithm improves image quality in craniocervical CT angiography. *AJR. American journal of roentgenology*. Dec 2013;201(6):W861-866.
92. Schaafsma JD, Velthuis BK, Vincken KL, de Kort GA, Rinkel GJ, Bartels LW. Artefacts induced by coiled intracranial aneurysms on 3.0-Tesla versus 1.5-Tesla MR angiography-An in vivo and in vitro study. *European journal of radiology*. May 2014;83(5):811-816.
93. Rinkel GJ, Wijndicks EF, Vermeulen M, et al. Nonaneurysmal perimesencephalic subarachnoid hemorrhage: CT and MR patterns that differ from aneurysmal rupture. *American Journal of Neuroradiology*. September 1, 1991 1991;12(5):829-834.
94. Kershenovich A, Rappaport ZH, Maimon S. Brain computed tomography angiographic scans as the sole diagnostic examination for excluding aneurysms in patients with perimesencephalic subarachnoid hemorrhage. *Neurosurgery*. Oct 2006;59(4):798-801; discussion 801-792.
95. Agid R, Andersson T, Almqvist H, et al. Negative CT angiography findings in patients with spontaneous subarachnoid hemorrhage: When is digital subtraction angiography still needed? *AJNR. American journal of neuroradiology*. Apr 2010;31(4):696-705.
96. Cruz JP, Sarma D, Noel de Tilly L. Perimesencephalic subarachnoid hemorrhage: when to stop imaging? *Emergency radiology*. Jun 2011;18(3):197-202.
97. MacKinnon AD, Clifton AG, Rich PM. Acute subarachnoid haemorrhage: is a negative CT angiogram enough? *Clinical radiology*. Mar 2013;68(3):232-238.
98. Lim LK, Dowling RJ, Yan B, Mitchell PJ. Can CT angiography rule out aneurysmal subarachnoid haemorrhage in CT scan-negative subarachnoid haemorrhage patients? *Journal of clinical neuroscience: official journal of the Neurosurgical Society of Australasia*. Jan 2014;21(1):191-193.